Quantum adiabatic optimization and combinatorial landscapes

V. N. Smelyanskiy,* S. Knysh,† and R. D. Morris‡
NASA Ames Research Center, MS 269-3, Moffett Field, California 94035-1000, USA
(Received 1 March 2004; published 16 September 2004)

In this paper we analyze the performance of the Quantum Adiabatic Evolution algorithm on a variant of the satisfiability problem for an ensemble of random graphs parametrized by the ratio of clauses to variables, $\gamma = M/N$. We introduce a set of macroscopic parameters (landscapes) and put forward an ansatz of universality for random bit flips. We then formulate the problem of finding the smallest eigenvalue and the excitation gap as a statistical mechanics problem. We use the so-called annealing approximation with a refinement that a finite set of macroscopic variables (*instead of* only energy) is used, and are able to show the existence of a dynamic threshold $\gamma = \gamma_d$ starting with some value of K—the number of variables in each clause. Beyond the dynamic threshold, the algorithm should take an exponentially long time to find a solution. We compare the results for extended and simplified sets of landscapes and provide numerical evidence in support of our universality ansatz. We have been able to map the ensemble of random graphs onto another ensemble with fluctuations significantly reduced. This enabled us to obtain tight upper bounds on the satisfiability transition and to recompute the dynamical transition using the extended set of landscapes.

DOI: 10.1103/PhysRevE.70.036702 PACS number(s): 05.10.−a, 02.50.−r, 05.70.−a, 05.90.+m

I. INTRODUCTION

An important open question in the field of quantum computing is whether it is possible to develop quantum algorithms capable of efficiently solving combinatorial optimization problems (COP). In the simplest case the task in a COP is to minimize the cost (energy) function E_σ with the domain given by the set of all possible assignments of N binary variables, $\boldsymbol{\sigma}=\{\sigma_1,\ldots,\sigma_N\}$, $\sigma_j=\pm 1$. The energy function possesses the locality property: it can be written as a sum of functions, each involving $O(1)$ binary variables. One example from physics is an Ising model, where the energy is given by the sum over pairs of interacting spins

$$E_{\boldsymbol{\sigma}} = \sum_{\langle ik\rangle} J_{ik}\sigma_i\sigma_k. \tag{1}$$

Another example from computer science is the satisfiability problem. Each term of the energy function involves $K = O(1)$ variables, and equals either 0 for combinations of variables that are allowed, or 1 for combinations that violate a constraint. The energy function then corresponds to the number of violated constraints and the task is to find an assignment of variables corresponding to $E=0$ or to show that no such assignment exists ($E_{\min}>0$). The satisfiability problem belongs to the huge class of hard *NP*-complete problems [1]. The time needed to solve these problems grows exponentially with N using the best known classical algorithms. The quantum computer emerges as a viable alternative, and whether *NP*-complete problems can be solved efficiently on a quantum computer is a central open question.

Connections between physics and computer science were made in seminal papers on simulated annealing [2] and the applications of methods of classical statistical mechanics [3] to optimization problems. Recently ideas from the replica theory of classical spin glasses were successfully applied to the design of novel algorithms [4]. It is only natural to extend this work to the quantum realm. Indeed, in the language of quantum computation the minimization of the cost function is equivalent to finding the ground state of a Hamiltonian $\mathcal{H}_P$,

$$\mathcal{H}_P = \sum_{\boldsymbol{\sigma}} E_{\boldsymbol{\sigma}} |\boldsymbol{\sigma}\rangle\langle\boldsymbol{\sigma}|, \tag{2}$$

where the summation is over the 2^N states $|\boldsymbol{\sigma}\rangle$ forming the computational basis of a quantum computer with N qubits.

A new family of quantum adiabatic evolution algorithms has been recently proposed by Farhi and co-workers [5,6]. This algorithm can be thought of as a quantum analogue of the simulated annealing algorithm. Numerical simulations were performed to study its performance for satisfiability problems [7]. Note that owing to the locality property, efficient implementation of these algorithms on a quantum computing device is feasible [5,8,9]. Simulations of quantum adiabatic evolution algorithms (QAA) for these *NP*-complete problems on a classical computer for randomly generated problem instances that are hard for classical algorithms were performed for small instances ($N \lesssim 25$) [6,7,10]. Results suggest a *quadratic* scaling law of the run time of the QAA with N. Recent experiments [11] on quantum annealing of the disordered ferromagnet $LiHo_xY_{1-x}F_4$ show that quantum annealing dramatically outperforms its classical counterpart, thermal annealing. Note that the experimental realization of the algorithm is not prone to finite-size artifacts that may cast doubt on results of computer simulations. In other Monte Carlo simulations of the quantum annealing algorithm on a classical computer, it was shown to be superior to thermal annealing [12]. Note that the performance increase would be much larger if quantum annealing were implemented on a quantum computing device. The general consensus is that the

*Electronic address: Vadim.N.Smelyanskiy@nasa.gov
†Electronic address: knysh@email.arc.nasa.gov
‡Electronic address: rdm@email.arc.nasa.gov

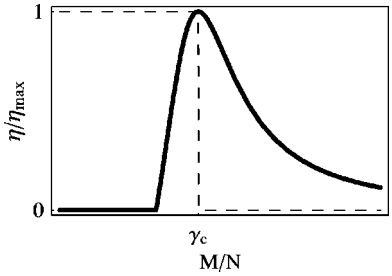

FIG. 1. Solid line shows the qualitative plot of the normalized quantity $\eta/\eta_{\max}$ vs M/N ($\eta_{\max}$ is a maximum value of η). Dashed line shows the proportion of satisfiable instances vs M/N.

speedup is due to the effects of quantum tunneling between states separated by high (but thin) barriers, impenetrable for systems obeying classical dynamics [6,11,13].

Despite evidence for advantages of QAA over traditional methods, no theoretical investigations into its performance were made except for simple models [14]. We choose to investigate this for a random hypergraph model, which is believed to describe real-world examples fairly well. In practice, algorithms for *NP*-complete problems are characterized by a wide range of running times, from linear to exponential, depending on the choice of certain control parameters of the problem (e.g., in satisfiability it is the ratio of the number of constraints to the number of variables, M/N). Therefore, a practically important alternative to the worst case complexity analysis is the study of a typical-case behavior of optimization algorithms on ensembles of randomly generated problem instances chosen from a given probability distribution. For the example of the Exact Cover problem considered in [6] (also called positive 1-in-3 SAT in [15]), one can define a uniform ensemble of random problem instances. For each one of M constraints we choose at random three variables, so that all combinations of variables have equal probability of $1/\binom{N}{3}$ and the constraints are statistically independent.

Anticipating an exponential scaling law for the algorithm's running times t_a it is convenient to analyze the distribution of a normalized logarithmic quantity $\log t_a/N$. This distribution becomes increasingly narrow in the limit of large N where the mean value $\langle \log t_a \rangle/N$ well characterizes the typical case exponential complexity of an algorithm. For the satisfiability problem the dependence of the asymptotic quantity

$$\eta = \lim_{N\to\infty} \langle \log t_a \rangle / N \tag{3}$$

on the clause-to-variable ratio $\gamma = M/N$ has the qualitative form shown in Fig. 1. At some critical value $\gamma = \gamma_d$ algorithmic complexity undergoes the dynamical transition from polynomial to exponential scaling law. This transition has been studied recently for the case of a variant of the classical random-walk algorithm for the satisfiability problem [16]. Function $\eta(\gamma)$ is nonmonotonic in γ and reaches its maximum at a certain point $\gamma_c > \gamma_d$. It was discovered some time ago [17–19] that γ_c is a critical value for the so-called satisfiability phase transition: if $\gamma < \gamma_c$, a randomly drawn instance is satisfiable with high probability, i.e., there exists at least one bit assignment $\boldsymbol{\sigma}$ that satisfies all the constraints ($E_{\boldsymbol{\sigma}}=0$). For $\gamma > \gamma_c$ instances are almost never satisfiable. In the asymptotic limit $N\to\infty$ the proportion of satisfiable instances drops from 1 to 0 infinitely steeply at $\gamma = \gamma_c$ as shown in Fig. 1.

The value of γ_d (unlike γ_c) depends on both the problem at hand and the optimization algorithm. Recent years have seen a growing interest in the study of dynamic threshold phenomena for local search algorithms [16,20]. That effort is in its initial stage and simple approximations (in the spirit of annealing approximations) were employed to estimate the location of the threshold. Comparison of the dynamical thresholds γ_d for different algorithms provides an important relative measure of their typical-case performance in a given problem.

This paper is organized as follows. In Sec. II we introduce the Quantum Adiabatic Evolution algorithm and explain how the complexity of the algorithm depends on the spectrum of the Hamiltonian. In Sec. III we formulate the quasiclassical approximation used to study the complexity and introduce the notion of landscapes. In Sec. IV we introduce positive K-NAE SAT and positive 1-in-K SAT—the *NP*-complete problems, which we use as a test-bed for our method. In Sec. V we provide detailed computation of entropy and landscapes within the annealing approximation. We discuss the universality of landscape probability distributions in Sec. VI. Sections VII and VIII are devoted to improving the annealing bound. A subgraph responsible for the hardest part of the problem (a core) is identified and results are rederived for the subgraph. In all cases we are concerned with finding the dynamic threshold—the critical ratio of clauses to variables above which the algorithm is expected to take an exponentially long time to find a solution. We discuss our results as well as possible ramifications and extensions of our work in the Conclusions (Sec. IX). In the Appendix we sketch a proof of *NP*-completeness of the problems considered.

II. QUANTUM ADIABATIC EVOLUTION ALGORITHM

Consider the time-dependent Hamiltonian $\mathcal{H}(t) \equiv \mathcal{H}(t/T)$,

$$\mathcal{H}(\tau) = (1-\tau)\mathcal{H}_B + \tau\mathcal{H}_P, \tag{4}$$

where $\tau = t/T \in (0,1)$ is dimensionless "time," $\mathcal{H}_P$ is the "problem" Hamiltonian (2) and $\mathcal{H}_B$ is a "driver" Hamiltonian, that is designed to cause transitions between the eigenstates of $\mathcal{H}_P$. Using dimensionless time and setting $\hbar = 1$ the quantum state evolution obeys the equation, $iT\partial|\Psi(\tau)\rangle/\partial\tau = \mathcal{H}(\tau)|\Psi(\tau)\rangle$. At the initial moment the quantum state $|\Psi(0)\rangle$ is prepared to be the ground state of $\mathcal{H}(0) = \mathcal{H}_B$. In the simplest case

$$\mathcal{H}_B = -\sum_{j=1}^{N} \sigma_x^j, \quad |\Psi(0)\rangle = 2^{-N/2}\sum_{\boldsymbol{\sigma}} |\boldsymbol{\sigma}\rangle, \tag{5}$$

where σ_x^j is a Pauli matrix for jth qubit. Consider the instantaneous eigenstates of $\mathcal{H}(\tau)$ with eigenvalues $\lambda_k(\tau)$ arranged in nondecreasing order at any value of $\tau \in (0,1)$,

$$\mathcal{H}(\tau)|\phi_k(\tau)\rangle = \lambda_k(\tau)|\phi_k(\tau)\rangle, \tag{6}$$

here $k=0,1,2,\ldots,2^N-1$. Provided the value of T (the runtime of the algorithm) is large enough and there is a finite gap for all $\tau\in(0,1)$ between the ground and excited state energies, $\lambda_1(\tau)-\lambda_0(\tau)>0$, the quantum evolution is adiabatic and the state of the system $|\Psi(\tau)\rangle$ stays close to an instantaneous ground state, $|\phi_0(\tau)\rangle$ (up to a phase factor). The state $|\phi_0(1)\rangle$ coincides with the ground state of the problem Hamiltonian $\mathcal{H}_P$ and, therefore, a measurement performed on the quantum computer at the final moment $t=T$ ($\tau=1$) will yield one of the solutions of the COP with large probability.

The standard criterion for adiabatic evolution is usually formulated in terms of minimum excitation gap between the ground and first excited states [21]

$$T \gg \frac{\mathcal{E}}{\Delta\lambda_{\min}^2}, \quad \Delta\lambda_{\min} = \max_{0\leqslant\tau\leqslant 1}[\lambda_1(\tau)-\lambda_0(\tau)]. \tag{7}$$

Here the quantity $\mathcal{E}$ is less than the largest eigenvalue of the operator $\mathcal{H}_P-\mathcal{H}_B$ [14] and scales polynomially with N in the problems we consider.

III. QUASICLASSICAL APPROXIMATION AND COMBINATORIAL LANDSCAPES

In the computational basis (2) we have

$$\mathcal{H} = \tau\sum_{\boldsymbol{\sigma}} E_{\boldsymbol{\sigma}}|\boldsymbol{\sigma}\rangle\langle\boldsymbol{\sigma}| - (1-\tau)\sum_{\boldsymbol{\sigma},\boldsymbol{\sigma}'}\delta[d(\boldsymbol{\sigma},\boldsymbol{\sigma}'),1]|\boldsymbol{\sigma}\rangle\langle\boldsymbol{\sigma}'|, \tag{8}$$

here $\delta[m,n]$ denotes the Kronecker delta-symbol and the summation is over the pairs of spin configurations $\boldsymbol{\sigma}$ and $\boldsymbol{\sigma}'$ that differ by the orientation of a single spin, $d(\boldsymbol{\sigma},\boldsymbol{\sigma}')=1$, where

$$d(\boldsymbol{\sigma},\boldsymbol{\sigma}') = \frac{1}{2}\sum_{j=1}^{N}|\sigma_j-\sigma_j'|, \tag{9}$$

denotes a so-called Hamming distance between the spin configurations $\boldsymbol{\sigma}$ and $\boldsymbol{\sigma}'$, that is the number of spins with opposite orientations. Equation (6) in the computational basis takes form

$$\lambda(\tau)\phi_{\boldsymbol{\sigma}}(\tau) = \tau E_{\boldsymbol{\sigma}}\phi_{\boldsymbol{\sigma}}(\tau) - (1-\tau)\sum_{\boldsymbol{\sigma}'}\delta[d(\boldsymbol{\sigma},\boldsymbol{\sigma}'),1]\phi_{\boldsymbol{\sigma}'}(\tau) \tag{10}$$

(here we drop the subscript indicating the number of a quantum state in λ and $\phi_{\boldsymbol{\sigma}}$). In what follows we assume that typical energies $E_{\boldsymbol{\sigma}}=O(N)$, but the change in the energy after a single spin flip is $O(1)$. This assumption about the energy landscape holds for instances of the satisfiability problem with the clause-to-variable ratio $M/N=O(1)$, the case of most interest for us (see the discussion in Sec. I).

We now consider a set of functions $\{X_l=C_l(\boldsymbol{\sigma},\mathcal{I}),\ l=1,\ldots,\mathcal{K}\}$, referred to as (combinatorial) landscapes, that depend on a problem instance $\mathcal{I}$ and project a spin configuration $\boldsymbol{\sigma}$ onto a vector $\{X_l\}$ with integer-valued components. Prior to considering a specific COP here we make certain assumptions about the properties of landscapes and apply them to the analysis of the minimum gap in the QAA.

In particular, we assume that, similar to energy, landscapes $\{X_l=C_l(\boldsymbol{\sigma},\mathcal{I})\}$ are macroscopic functions, so that the typical values of X_l are $O(N)$, and possess a certain *universality* property in the asymptotic limit $N\to\infty$. Specifically, the joint distribution of $\{C_l(\boldsymbol{\sigma},\mathcal{I})\}$ over the spin configurations $\boldsymbol{\sigma}$ forming the 1-spin-flip neighborhood of an "ancestor" configuration $\boldsymbol{\sigma}'$ depends on a problem instance $\mathcal{I}$ and spin configuration $\boldsymbol{\sigma}'$ *only* via the set of parameters $\{X_l'=C_l(\boldsymbol{\sigma}',\mathcal{I})\}$. We then define a quantity

$$P(\{X_l\}|\{X_l'\}) = \frac{1}{N}\sum_{d(\boldsymbol{\sigma},\boldsymbol{\sigma}')=1}\prod_{k=1}^{\mathcal{K}}\delta[X_l,C_l(\boldsymbol{\sigma},\mathcal{I})],$$

$$X_l' = C_l(\boldsymbol{\sigma}',\mathcal{I}). \tag{11}$$

In effect, the above universality property of landscapes implies that the set of all possible spin configurations $\boldsymbol{\sigma}$ is divided into "boxes" with coordinates $\{X_l\}$ where $X_l=C_l(\boldsymbol{\sigma})$, and $P(\{X_l\}|\{X_l'\})$ (11) represents the transition probability from box $\{X_l\}$ to box $\{X_l'\}$. In particular, it obeys Bayes' rule

$$P(\{X_l\}|\{X_l'\})\Omega(\{X_l'\}) = P(\{X_l'\}|\{X_l\})\Omega(\{X_l\}), \tag{12}$$

where $\Omega(\{X_l\})$ is the number of different spin configurations in the box $\{X_l\}$.

We consider energy to be a smooth function of landscapes

$$E_{\boldsymbol{\sigma}} = E(\{X_l\}), \quad X_l \equiv C_l(\boldsymbol{\sigma},\mathcal{I}), \tag{13}$$

so that $|\partial E/\partial X_l|=O(1)$. Furthermore, we assume that, on one hand, the change in $C_l(\boldsymbol{\sigma},\mathcal{I})$ after flipping one spin is $O(1)$, for typical problem instances. On the other hand, we assume that correlation properties in a neighborhood of a box $\{X_l\}$ described by $P(\{X_l\}|\{X_l'\})$ vary smoothly with box coordinates on a scale $1\lesssim|\delta X_l|\ll N$. Therefore if we write the transition probability in the form

$$P(\{X_l'\}|\{X_l\}) = p(\{X_l'-X_l\};\{x_l\}), \quad \{x_l\equiv X_l/N\}, \tag{14}$$

then $p(\{k_l\};\{x_l\})$ is a steep function of its first argument: it decays rapidly in the range $1\lesssim|k_l|\ll N$ for each l-component. However this is a smooth function of its second argument: it varies slightly when coordinates x_l change on a scale $|\delta x_l|\ll 1$.

One can show that under the above assumptions the quantum amplitudes $\phi_{\boldsymbol{\sigma}}$ corresponding to the smallest eigenvalue depend on the spin configuration $\boldsymbol{\sigma}$ only via the coordinates of this box $\{X_l\}$ to which it belongs. Then we look for the solution of Eq. (10) in the following form:

$$\phi_{\boldsymbol{\sigma}}(\tau) = \frac{\varphi(\{X_l\},\tau)}{\sqrt{\Omega(\{X_l\})}}, \quad \{X_l\equiv C_l(\boldsymbol{\sigma},\mathcal{I})\}, \tag{15}$$

where $|\varphi(\{X_l\},\tau)|^2$ gives the probability of finding the system in the box $\{X_l\}$. Plugging Eq. (15) into Eq. (10) and making use of Eqs. (12) and (13) we obtain:

$$\lambda(\tau)\varphi(\mathbf{X},\tau) = \tau E(\mathbf{X})\varphi(\mathbf{X},\tau) - (1-\tau)N\sum_{\mathbf{X}'} L(\mathbf{X},\mathbf{X}'\})\varphi(\mathbf{X}',\tau), \tag{16}$$

$$\mathbf{X} \equiv \{X_1, X_2, \ldots, X_K\} \tag{17}$$

(hereafter we use the above shorthand notation for the set of landscapes). In (16) we introduced

$$L(\mathbf{X},\mathbf{X}') = L(\mathbf{X}',\mathbf{X}) = P(\mathbf{X}'|\mathbf{X})\sqrt{\frac{P(\mathbf{X})}{P(\mathbf{X}')}},$$

$$P(\mathbf{X}) = 2^{-N}\Omega(\mathbf{X}), \tag{18}$$

where $P(\mathbf{X})$ is a probability that a randomly sampled configuration $\boldsymbol{\sigma}$ belongs to a box $\mathbf{X}$. We shall look for a solution of (16) in the WKB-like form

$$\varphi(\mathbf{X},\tau) = \exp[-W(\mathbf{X},\tau)], \tag{19}$$

so that

$$\lambda(\tau) = \tau E(\mathbf{X}) - (1-\tau)N\sum_{\mathbf{X}'} L(\mathbf{X},\mathbf{X}')e^{W(\mathbf{X},\tau)-W(\mathbf{X}',\tau)}. \tag{20}$$

We now introduce scaled variables [cf. (14)]

$$\mathbf{x} = \frac{\mathbf{X}}{N}, \quad \Gamma = \frac{1-\tau}{\tau}, \quad g = \frac{\lambda}{\tau N}, \tag{21}$$

and also

$$w(\mathbf{x},\Gamma) \equiv \frac{1}{N}W(\mathbf{X},\tau), \quad \varepsilon(\mathbf{x}) \equiv \frac{1}{N}E(\mathbf{X}), \quad s(\mathbf{x}) \equiv \frac{1}{N}\log\Omega(\mathbf{X}), \tag{22}$$

where $s(\mathbf{x})$ is an entropy function. Based on (18) and the properties of the transition probability [see Eq. (14) and the discussion after it] we assume that the sum over $\mathbf{X}'$ in (20) is dominated by terms with $|\mathbf{X}'-\mathbf{X}| = O(1)$. Then we can use an approximation

$$W(\mathbf{X}',\tau) - W(\mathbf{X},\tau) \approx \nabla w \cdot (\mathbf{X}'-\mathbf{X}) + O(1/N), \tag{23}$$

where $\nabla w \equiv \partial w(\mathbf{x},\boldsymbol{\Gamma})/\partial\mathbf{x}$. Plugging (23) into (20) and making use of Eqs. (14), (18), (21), and (22) we obtain after some transformations:

$$g = h(\mathbf{x},\nabla w;\Gamma),$$

$$h(\mathbf{x},\mathbf{p};\Gamma) = \varepsilon(\mathbf{x}) - \Gamma\sum_{\mathbf{k}} p(\mathbf{k};\mathbf{x})e^{-\mathbf{k}\cdot(\nabla s/2+\mathbf{p})} \tag{24}$$

[here $\nabla s \equiv \partial s(\mathbf{x})/\partial\mathbf{x}$]. This is a Hamilton-Jacobi equation for an auxiliary mechanical system with coordinates $\mathbf{x}$, momenta $\mathbf{p} = \nabla w$, action w, Hamiltonian function $h(\mathbf{x},\mathbf{p};\Gamma)$ and energy g. Using the symmetry relation

$$p(\mathbf{k};\mathbf{x})e^{-\mathbf{k}\cdot\nabla s/2} = p(-\mathbf{k};\mathbf{x})e^{\mathbf{k}\cdot\nabla s/2}, \tag{25}$$

that follows directly from Eqs. (12) and (18) we obtain that the minimum of $w(\mathbf{x},\Gamma)$ over $\mathbf{x}$ where $\nabla w = 0$ necessarily corresponds to the minimum of the functional:

$$f(\mathbf{x},\Gamma) = \varepsilon(\mathbf{x}) - \Gamma\ell(\mathbf{x}), \tag{26}$$

where $f(\mathbf{x},\Gamma) \equiv h(\mathbf{x},\mathbf{0},\Gamma)$ and

$$\ell(\mathbf{x}) = \tilde{p}(\nabla s/2;\mathbf{x}), \quad \tilde{p}(\mathbf{y};\mathbf{x}) \equiv \sum_{\mathbf{k}} p(\mathbf{k};\mathbf{x})e^{-\mathbf{k}\cdot\mathbf{y}}. \tag{27}$$

The summation in (24) and (27) is over components k_l of $\mathbf{k}$ in the range $k_l \in (-\infty,\infty)$. In what follows, we shall refer to $\tilde{p}(\mathbf{y};\mathbf{x})$ in (27) as a "Laplace transform" of $p(\mathbf{k};\mathbf{x})$.

We note that $\ell(\mathbf{x}) = \Sigma_{\mathbf{x}'} L(\mathbf{X}',\mathbf{X})$ and one can use Bayes rule and the Cauchy-Bunyakovsky inequality in (18) to show that that the positive-valued function $\ell(\mathbf{x})$ is bounded from above, $0 < \ell(\mathbf{x}) \leqslant 1$. This shows that the analysis of the effective potential based on the WKB approximation (23) is self-consistent in the asymptotic limit $N \to \infty$.

It follows from the above analysis that the ground-state wave function $\psi(\mathbf{x},\Gamma) \equiv \varphi(\mathbf{X},\tau)$ is concentrated in $\mathbf{x}$-space near the bottom of the "effective potential" given by the functional $f(\mathbf{x},\Gamma)$, i.e., near the point $\mathbf{x}_*(\Gamma)$ where $f(\mathbf{x},\Gamma)$ reaches its minimum. In this region $S \approx 1/2\mathbf{x}^T\hat{\mathbf{A}}\mathbf{x}$, where matrix $\hat{\mathbf{A}}$ is positive definite, and according to (19), the wave function has a Gaussian form with width $\propto 1/\sqrt{N}$.

The ground-state energy $g \equiv g(\Gamma)$ is given by the value of the effective potential f (26) at its minimum

$$g(\Gamma) = f(\mathbf{x}_*(\Gamma),\Gamma),$$

$$\partial f(\mathbf{x},\Gamma)/\partial\mathbf{x}|_{\mathbf{x}=\mathbf{x}_*(\Gamma)} = 0, \quad f(\mathbf{x},\Gamma) \geqslant g(\Gamma). \tag{28}$$

We note that as $\Gamma \to 0$ the shape of the effective potential $f(\mathbf{x},\Gamma)$ approaches that of the energy function $\varepsilon(\mathbf{x})$ and therefore its minimum $\mathbf{x}_*(\Gamma) \to \mathbf{x}_0$ where $\mathbf{x}_0$ is a minimum of $\varepsilon(\mathbf{x})$. It can be shown that in this limit the ground-state eigenvalue approaches the minimum energy value $\varepsilon(\mathbf{x}_0)$ and the eigenvalues of $\mathbf{A}^{-1}$ approach zero [and so does the characteristic width of the wavepacket $\psi(\mathbf{x},\Gamma)$]. The spin configurations that belong to a box $\mathbf{x}_0$ in $\mathbf{x}$-space correspond to the solutions of the optimization problem at hand. It is clear that one of the solutions can be recovered with high probability after a measurement is performed at the end of the "quantum annealing" procedure.

Variational ansatz: For cases in which the set of macroscopic variables $\{X_l\}$ is not sufficient [in a statistical sense (14)] to describe the dynamics of the quantum algorithm, one can still implement the above procedure as an *approximation*, using a variational method. Introducing a Lagrangian multiplier λ, one looks for the minimum of the functional $F(\varphi,\lambda) = \langle\phi|\mathcal{H}|\phi\rangle - \lambda(\langle\phi|\phi\rangle - 1)$, using a variational ansatz (15) for the wave function. The solution of the variational problem is provided by Eqs. (19)–(28). The smallest eigenvalue g (28) corresponds to the value of the Lagrange multiplier at the extremum, $\lambda = \tau N g$, and the maximum of the variational wave function corresponds to the minimum of the effective potential f (26).

Global bifurcations of the effective potential. However, in the case of a global bifurcation where the effective potential $f(\mathbf{x},\Gamma)$ possesses degenerate or nearly degenerate global

minima, the answer is modified. If for some value of $\Gamma=\Gamma_*$, a global bifurcation occurs, in our example this would mean that for this value of Γ, two values of $\mathbf{x}$, $\mathbf{x}_*^+$ and $\mathbf{x}_*^-$ give a global minimum to $f(\mathbf{x},\Gamma)$. In such a case, the smallest eigenvalue is not doubly degenerate; rather an exponentially small gap $\Delta\lambda_{\min}$ between the ground and first excited state is developed, itself being proportional to the overlap between two wave functions, peaked around $\mathbf{x}_*^+$ and $\mathbf{x}_*^-$, respectively.

To estimate the overlap we note that at Γ_* the two global minima of the effective potential $f(\mathbf{x},\Gamma_*)$ correspond to the two coexisting fixed points of the Hamiltonian function in (24) with zero momentum and the same values of energy g,

$$\partial f/\partial \mathbf{x} = \partial h/\partial \mathbf{x} = \partial h/\partial \mathbf{p} = 0, \tag{29}$$

$$\mathbf{x} = \mathbf{x}_*^{\pm}, \quad \mathbf{p} = \mathbf{p}_*^{\pm} = \mathbf{0}, \quad g(\mathbf{x},\mathbf{p};\Gamma_*) = g_*^+ = g_*^-. \tag{30}$$

Then to logarithmic accuracy we have

$$\frac{1}{N}\log \Delta g_{\min} = \int_{-\infty}^{\infty} dt' [\dot{\mathbf{x}}(t')\mathbf{p}(t') - h(\mathbf{x}(t'),\mathbf{p}(t'))] + O(1/N), \tag{31}$$

where $(\mathbf{x}(t),\mathbf{p}(t))$ is a heteroclinic trajectory connecting the two fixed points of (24)

$$\dot{\mathbf{x}}(t) = \partial h/\partial \mathbf{p}, \quad \dot{\mathbf{p}}(t) = -\partial h/\partial \mathbf{x},$$

$$\mathbf{x}(t \to \pm\infty) = \mathbf{x}_*^{\pm}, \quad \mathbf{p}(t \to \pm\infty) = \mathbf{0}. \tag{32}$$

From the algorithmic perspective this means that when Γ gets close to Γ_*, it has to change exponentially slowly [cf. Sec. II and Eq. (7)]. This could be called a critical slowing down in the vicinity of a quantum phase transition. If simulated annealing (SA) is used and a similar phenomenon occurs, the value of the temperature T_* is the point where a global bifurcation occurs in the free energy functional

$$f(\mathbf{x},T) = \varepsilon(\mathbf{x}) - Ts(\mathbf{x}). \tag{33}$$

By comparing the free energy functional (33) with the functional (26) corresponding to "quantum annealing" (QA), we note that in QA the quantities Γ and $\ell(\mathbf{x})$ play the roles of temperature and entropy in SA, respectively.

We note in passing that a similar picture for the onset of global bifurcation that can lead to the failure of QA and (or) SA was proposed in [14,22] for the case where the energy $E_{\boldsymbol{\sigma}}$ is a nonmonotonic function of a single landscape parameter, a total spin $\Sigma_{j=1}^N \sigma_j$. In this case the dynamics of QA can be described in terms of one-dimensional effective potential [23,24].

IV. THE MODELS

An instance of a satisfiability problem with N binary variables committed to $M=\gamma N$ constraints (where each constraint is a clause involving K variables) can be defined by the specification of the following two objects. One of them is an $M\times N$ matrix $\hat{\mathcal{G}}$, the rows of the matrix are independent K-tuples of distinct bit indexes sampled from the interval $(1,N)$. The mth row of $\hat{\mathcal{G}}$ defines the subset of the K binary variables involved in the mth clause. The second object is a set of boolean functions $\mathcal{B}=\{\boldsymbol{b}_m\}$, with each function encoding a corresponding constraint. A function $\boldsymbol{b}_m = \boldsymbol{b}_m[\sigma_{\mathcal{G}_{m1}},\sigma_{\mathcal{G}_{m2}},\ldots,\sigma_{\mathcal{G}_{mK}}]$ is defined over the set of 2^K possible assignments of the string of K binary variables involved in the mth clause. The function returns value 1 for assignments of binary variables that satisfy the constraint and 0 for bit assignments that violate it. Then the energy function equals to the number of violated constraints

$$E_{\boldsymbol{\sigma}} \equiv E_{\boldsymbol{\sigma}}(\mathcal{I}) = M - \sum_{m=0}^{M} \boldsymbol{b}_m[\boldsymbol{\sigma}_{\mathcal{G}_{m1}},\sigma_{\mathcal{G}_{m2}},\ldots,\sigma_{\mathcal{G}_{mK}}], \tag{34}$$

here $\mathcal{I}=(\mathcal{G},\mathcal{B})$ denotes an instance of a problem.

The matrix $\hat{\mathcal{G}}$ defines a hypergraph $\mathcal{G}$ that is made up of the set of N vertices (corresponding to the variables in the problem) and a set of M hyperedges (corresponding to the constraints of the problem), each one connecting K vertices. An ensemble of *disorder configurations* of the hypergraph corresponds to all the possible ways one can place $M=\gamma N$ hyperedges among N vertices where each hyperedge carries K vertices. Under the uniformity ansatz all configurations of disorder are sampled with equal probability [i.e., rows of the matrix $\hat{\mathcal{G}}$ are independently and uniformly sampled in the $(1,N)$ interval].

Boolean functions b_m may also be generated at random for each constraint with an example being random K-SAT problem [25,26]. However here we consider slightly different versions of the random satisfiability problem that are still defined on a random hypergraph $\mathcal{G}$ but have a nonrandom boolean function $\boldsymbol{b}_m=\boldsymbol{b}$, identical for all the clauses in a problem. One of the problems is Positive 1-in-K SAT in which a constraint is satisfied if and only if exactly one bit is equal to 1 and the other $K-1$ bits are equal to 0. The boolean function $\boldsymbol{b}$ for this problem takes the form

$$\mathbf{b}[\alpha_1,\alpha_2,\ldots,\alpha_K] = \delta\left[\sum_{p=1}^{K}\frac{1-\alpha_p}{2},1\right] \quad \text{(Positive 1-in-}K\text{ SAT)}. \tag{35}$$

$$\alpha_p = \pm 1, \quad p = 1,2,\ldots,K.$$

We shall also consider another problem, Positive K-NAE-SAT, in which a clause is satisfied unless all variables that appear in a clause are equal ("K-Not-All-Equal-SAT"). The boolean function $\boldsymbol{b}$ for this problem takes the form

$$\boldsymbol{b}[\alpha_1,\alpha_2,\ldots,\alpha_K] = 1 - \sum_{s=\pm 1}\delta\left[\sum_{p=1}^{K}\frac{1+s\alpha_p}{2},0\right] \quad \text{(Positive } K\text{ NAE-SAT)}. \tag{36}$$

Both problems are *NP*-complete (Appendix). It will be shown below that they are characterized by the same set of landscape functions.

V. LANDSCAPES: ANNEALING APPROXIMATION

For a particular spin ($\boldsymbol{\sigma}$) and disorder ($\mathcal{G}$) configurations, all clauses can be divided into 2^K distinct groups according to the values of the binary variables that appear in a clause. We will label the different types of clauses by vectorial index $\boldsymbol{\alpha}=\{\alpha_1,\ldots,\alpha_K\}$, $\alpha_p=\pm 1$. We now divide the set of 2^N spin configurations into boxes identified by certain numbers of clauses of each type, $N\mathcal{M}_{\boldsymbol{\alpha}}$, and also by the Ising spin in a configuration N_q,

$$\mathcal{M}_{\boldsymbol{\alpha}} \equiv \mathcal{M}_{\boldsymbol{\alpha}}(\boldsymbol{\sigma},\mathcal{G}) = \frac{1}{N}\sum_{m=1}^{M}\prod_{p=1}^{K}\delta[\sigma_{\mathcal{G}_{mp}},\alpha_p], \tag{37}$$

$$q \equiv q(\boldsymbol{\sigma}) = \frac{1}{N}\sum_{j=1}^{N}\sigma_j. \tag{38}$$

Different boxes correspond to macroscopic states defined by the set of parameters $(q,\{\mathcal{M}_{\boldsymbol{\alpha}}\})$ with $q\in(-1,1)$ and $\Sigma_{\boldsymbol{\alpha}}\mathcal{M}_{\boldsymbol{\alpha}}=\gamma$. The energy function can be expressed via (37) as follows [cf. (34)–(36)]:

$$\begin{aligned}\varepsilon(\{\mathcal{M}_{\boldsymbol{\alpha}}\}) &= \gamma - \sum_{m=0}^{K}\zeta_m M_m,\\ \mathcal{M}_m &\equiv \sum_{\boldsymbol{\alpha}}\mathcal{M}_{\boldsymbol{\alpha}}\delta\left[K-2m,\sum_{p=1}^{K}\alpha_p\right],\end{aligned} \tag{39}$$

where the form of the coefficients ζ_m depends on the problem:

$$\zeta_m = \begin{cases}\delta[m,1] & \text{(Positive 1-in-}K\text{ SAT)}\\ 1-\delta[m,0]-\delta[m,K] & \text{(Positive }K\text{-NAE-SAT)}.\end{cases} \tag{40}$$

In the following we compute an approximation to the effective potential (26), using the landscape functions (37) and (38). According to (27) it depends on the entropy function $s(q,\{\mathcal{M}_{\boldsymbol{\alpha}}\})$ and the transition probability (14) between different macroscopic states. Recalling that variables q and $\mathcal{M}_{\boldsymbol{\alpha}}$ are normalized by the factor N we study the probability of transition, $p(n,\{r_{\boldsymbol{\alpha}}\};q,\{\mathcal{M}_{\boldsymbol{\alpha}}\})$, from the state $(q,\{\mathcal{M}_{\boldsymbol{\alpha}}\})$ to the state $(q+n/N,\{\mathcal{M}_{\boldsymbol{\alpha}}+r_{\boldsymbol{\alpha}}/N\})$. The Laplace transform of p with respect to $n,\{r_{\boldsymbol{\alpha}}\}$ has the form [cf. (27)]

$$\tilde{p}(\theta,\{y_{\boldsymbol{\alpha}}\};q,\{\mathcal{M}_{\boldsymbol{\alpha}}\}) = \sum_{n,\{r_{\boldsymbol{\alpha}}\}} e^{-\theta n-\Sigma_{\boldsymbol{\alpha}} y_{\boldsymbol{\alpha}} r_{\boldsymbol{\alpha}}} p(n,\{r_{\boldsymbol{\alpha}}\};q,\{\mathcal{M}_{\boldsymbol{\alpha}}\}). \tag{41}$$

We assume that all binary variables are also subdivided into distinct groups based on their value $\sigma=\pm 1$ and a vector $\mathbf{k}$ with integer coefficients $k^p_{\boldsymbol{\alpha}}$ indicating the number of times a variable appears in a clause of type $\boldsymbol{\alpha}$ in position p. Clearly, consistency requires that $k^p_{\boldsymbol{\alpha}}=0$ unless $\boldsymbol{\alpha}_p=\sigma$. We now define a quantity $c_{\sigma,\mathbf{k}}$ which is equal to the fraction of spins with given $\sigma,\mathbf{k}$. For a spin configuration $\boldsymbol{\sigma}$ there exists a set of coefficients $\{c_{\sigma,\mathbf{k}}\}$ with elements of the set corresponding to all possible values of σ and $\mathbf{k}$ (there will be many 0's in a set for each spin configuration). In general, there are exponentially many sets $\{c_{\sigma,\mathbf{k}}\}$ that correspond to a macroscopic state $(q,\{\mathcal{M}_{\boldsymbol{\alpha}}\})$

$$\sum_{\sigma,\mathbf{k}}\sigma c_{\sigma,\mathbf{k}} = q, \quad \sum_{\sigma,\mathbf{k}} k^p_{\boldsymbol{\alpha}} c_{\sigma,\mathbf{k}} = \mathcal{M}_{\boldsymbol{\alpha}}\ \ (p=0,1,\ldots,K). \tag{42}$$

Coefficients $\{c_{\sigma,\mathbf{k}}\}$ are concentrations of spin variables with different types of "neighborhoods." We shall assume that in the limit of large N the distribution of coefficients $c_{\sigma,\mathbf{k}}$ corresponding to the same macroscopic state (42) is sharply peaked around their mean values (with the width of the distribution $\propto N^{-1/2}$).

Under the above assumption we can immediately compute the Laplace-transformed transition probability (41) in terms of the coefficients $c_{\sigma,\mathbf{k}}$. Indeed, consider flipping a spin with value σ and neighborhood type given by vector $\mathbf{k}$. This will change the total spin by -2σ and for each clause of type $\boldsymbol{\alpha}$ and index $p\in(1,K)$ the value of $N\mathcal{M}_{\boldsymbol{\alpha}}$ will decrease by $k^p_{\boldsymbol{\alpha}}$. On the other hand, for the clause type $\boldsymbol{\alpha}'\equiv\overline{\boldsymbol{\alpha}}(p,\boldsymbol{\alpha})$ obtained by flipping a bit in pth position in $\boldsymbol{\alpha}$, $N\mathcal{M}_{\boldsymbol{\alpha}'}$ is correspondingly increased by $k^p_{\boldsymbol{\alpha}}$. Hence the Laplace-transformed transition probability is

$$\tilde{p}(\theta,\{y_{\boldsymbol{\alpha}}\};q,\{\mathcal{M}_{\boldsymbol{\alpha}}\}) = \sum_{\sigma,\mathbf{k}} c_{\sigma,\mathbf{k}}\exp\left[2\theta\sigma+\sum_{p,\boldsymbol{\alpha}}(y_{\boldsymbol{\alpha}}-y_{\overline{\boldsymbol{\alpha}}(p,\boldsymbol{\alpha})})k^p_{\boldsymbol{\alpha}}\right], \tag{43}$$

where the coefficients $c_{\sigma,\mathbf{k}}$ are set to their mean values in a macroscopic state (42).

A. Entropy and coefficients $c_{\sigma,\mathbf{k}}$ in a macroscopic state defined by q and $\{\mathcal{M}_{\boldsymbol{\alpha}}\}$

Here we use the annealing approximation to estimate the mean values of $c_{\sigma,\mathbf{k}}$ and also of a macroscopic state $(q,\mathcal{M}_{\boldsymbol{\alpha}})$. We start by introducing the concept of annealed entropy. Let $\mathcal{N}$ be the number of spin configurations subject to some constraints. In general, it is a function of the disorder realization. The annealed entropy is defined as the logarithm of its disorder average: $s_{\text{ann}}=\ln\langle\mathcal{N}\rangle$. Note that for the correct, quenched, entropy the order of taking a logarithm and disorder average is reversed.

Since in the random hypergraph model all disorder configurations are equally probable, annealed entropy is given as $s_{\text{ann}}=\ln\mathcal{N}_{S,\mathcal{G}}-\ln\mathcal{N}_{\mathcal{G}}$, where $\mathcal{N}_{S,\mathcal{G}}$ is the total number of spin and disorder configurations and $\mathcal{N}_{\mathcal{G}}$ is the number of disorder configurations.

For enumerating all possible disorder configurations we depart slightly from the traditional random hypergraph model. In our model all clauses are ordered (two disorder configurations where any two clauses are permuted are deemed different); clauses can be repeated (the same clause can appear twice); the order of variables in a clause is important (two disorder configurations are different if the order of variables in any clause is changed); and finally, variables can be repeated in a single clause. This change does not alter the underlying physics, since the probability that two identical clauses appear is infinitesimal, and a variable enters a clause twice in at most $O(1)$ clauses, which can be safely neglected. As regards the distinction between the disorders

with permuted clauses, this only introduces a combinatorial factor which cancels out. The advantage is that each disorder can be represented as a sequence of M K-tuples of integers from 1 to N.

We will first compute the annealed entropy of a macroscopic state $(q,\{\mathcal{M}_{\boldsymbol{\alpha}}\})$ under additional constraints: we fix the values $c_{\sigma,\mathbf{k}}$ and compute the annealed entropy as a function of $q,\{\mathcal{M}_{\boldsymbol{\alpha}}\},\{c_{\sigma,\mathbf{k}}\}$. Recalling that $\mathcal{M}_{\boldsymbol{\alpha}}$ are the numbers of clauses of a given type scaled by N, and the total number of clauses is γN, we obtain the number of joint spin-disorder configurations as a product of the following factors:

(i) the number of ways to assign types to clauses $(N\gamma)!/\Pi_{\boldsymbol{\alpha}}(N\mathcal{M}_{\boldsymbol{\alpha}})!$,

(ii) the number of ways to assign types to variables $N!/\Pi_{\sigma,\mathbf{k}}(Nc_{\sigma,\mathbf{k}})!$,

(iii) for all p, $\boldsymbol{\alpha}$, the number of ways to permute the appearance of variables in pth position of clauses of type $\boldsymbol{\alpha}$: $(N\mathcal{M}_{\boldsymbol{\alpha}})!/\Pi_{\sigma,\mathbf{k}}(k^p_{\boldsymbol{\alpha}}!)^{Nc_{\sigma,\mathbf{k}}}$.

Consequently, the annealed entropy is given by

$$s_{\mathrm{ann}}[\{c_{\sigma,\mathbf{k}}\};q,\{\mathcal{M}_{\boldsymbol{\alpha}}\}] = -\sum_{\sigma,\mathbf{k}} c_{\sigma,\mathbf{k}} \ln\left[c_{\sigma,\mathbf{k}}\prod_{p,\boldsymbol{\alpha}}(k^p_{\boldsymbol{\alpha}}!)\right] + (K-1)\sum_{\boldsymbol{\alpha}}\mathcal{M}_{\boldsymbol{\alpha}}\ln\mathcal{M}_{\boldsymbol{\alpha}} + \gamma\ln\gamma - \gamma K. \tag{44}$$

In the large N limit we replace $c_{\sigma,\mathbf{k}}$ by their annealed averages, i.e., the values that maximize the annealed entropy. In its simplest form, we place no constraints on $c_{\sigma,\mathbf{k}}$ except consistency requirements (42). Associating Lagrange multipliers λ and $\ln\mu^p_{\boldsymbol{\alpha}}$ with these constraints, the expression for the entropy can be rewritten as

$$s_{\mathrm{ann}}[q,\{\mathcal{M}_{\boldsymbol{\alpha}}\}] = \min_{\lambda,\mu^p_{\boldsymbol{\alpha}}}\left\{-\lambda q + \sum_{p,\boldsymbol{\alpha}}\mathcal{M}_{\boldsymbol{\alpha}}\ln\frac{\mathcal{M}_{\alpha}}{\mu^p_{\boldsymbol{\alpha}}} + \ln Z[\lambda,\{\mu^p_{\boldsymbol{\alpha}}\}]\right\} - \sum_{\boldsymbol{\alpha}}\mathcal{M}_{\boldsymbol{\alpha}}\ln M_{\boldsymbol{\alpha}} + \gamma\ln\gamma - \gamma K. \tag{45}$$

The values of $c_{\sigma,\mathbf{k}}$ are given by

$$c_{\sigma,\mathbf{k}} = \frac{1}{Z}e^{\lambda\sigma}\prod_{p,\boldsymbol{\alpha}}(\mu^p_{\boldsymbol{\alpha}})^{k^p_{\alpha}/k^p_{\boldsymbol{\alpha}}!}, \tag{46}$$

and Z is given by

$$Z = \exp\left(\lambda + \sum_{\boldsymbol{\alpha}}\sum_{p}\delta[\boldsymbol{\alpha}_p,1]\mu^p_{\boldsymbol{\alpha}}\right) + \exp\left(-\lambda + \sum_{\boldsymbol{\alpha}}\sum_{p}\delta[\boldsymbol{\alpha}_p,-1]\mu^p_{\boldsymbol{\alpha}}\right). \tag{47}$$

The values of the Lagrange multipliers λ, $\mu^p_{\boldsymbol{\alpha}}$ are related to $q,\{\mathcal{M}_{\boldsymbol{\alpha}}\}$ via

$$\frac{\partial\ln Z}{\partial\lambda} = q, \tag{48}$$

$$\mu^p_{\boldsymbol{\alpha}}\frac{\partial\ln Z}{\partial\mu^p_{\boldsymbol{\alpha}}} = \mathcal{M}_{\boldsymbol{\alpha}}. \tag{49}$$

From here we obtain the expression for the Lagrange multiplier $\mu^p_{\boldsymbol{\alpha}}$,

$$\frac{\mathcal{M}_{\boldsymbol{\alpha}}}{\mu^p_{\boldsymbol{\alpha}}} = \frac{1+\boldsymbol{\alpha}_p q}{2}. \tag{50}$$

Then introducing a new notation

$$\mu_{\pm} = \sum_{p,\boldsymbol{\alpha}}\frac{1\pm\boldsymbol{\alpha}_p}{2}\mu^p_{\boldsymbol{\alpha}},$$

$$\mathcal{M}_{\pm} = \sum_{p,\boldsymbol{\alpha}}\frac{1\pm\boldsymbol{\alpha}_p}{2}\mathcal{M}_{\boldsymbol{\alpha}}, \tag{51}$$

we obtain

$$Z = e^{\lambda}e^{\mu_+} + e^{-\lambda}e^{\mu_-}, \quad \mu_{\pm} = \frac{2\mathcal{M}_{\pm}}{1\pm q}. \tag{52}$$

Then the entropy can be rewritten in the following form:

$$s_{\mathrm{ann}}[q,\{\mathcal{M}_{\boldsymbol{\alpha}}\}] = -\lambda q + \mathcal{M}_+\ln\frac{1+q}{2} + \mathcal{M}_-\ln\frac{1-q}{2} + \ln Z - \sum_{\boldsymbol{\alpha}}\mathcal{M}_{\boldsymbol{\alpha}}\ln\mathcal{M}_{\boldsymbol{\alpha}} + \gamma\ln\gamma - \gamma K. \tag{53}$$

We now use

$$e^{\lambda}e^{\mu_+} = Z\frac{1+q}{2}, \quad e^{-\lambda}e^{\mu_-} = Z\frac{1-q}{2} \tag{54}$$

and obtain the expression for the second Lagrange multiplier λ,

$$-\lambda q = -\frac{1+q}{2}\ln\frac{1+q}{2} - \frac{1-q}{2}\ln\frac{1-q}{2} - \ln Z + \gamma K. \tag{55}$$

Upon substitution of λ from the above into the expression for s_{ann} (53) we finally obtain the annealed entropy

$$s_{\mathrm{ann}}[q,\{\mathcal{M}_{\boldsymbol{\alpha}}\}] = -q\tanh^{-1}q - \ln\frac{\sqrt{1-q^2}}{2} + \mathcal{M}_+\ln\frac{1+q}{2} + \mathcal{M}_-\ln\frac{1-q}{2} - \sum_{\boldsymbol{\alpha}}\mathcal{M}_{\boldsymbol{\alpha}}\ln\mathcal{M}_{\boldsymbol{\alpha}} + \gamma\ln\gamma. \tag{56}$$

Also the coefficients $c_{\sigma,\mathbf{k}}$ are given by (46) and (47) with Lagrange multipliers given in (50) and (55).

B. Effective potential

Consider a factor $\ell(\mathbf{x}) = (\partial f/\partial\Gamma)_{\varepsilon}$ (26) and (27) in the expression (26) for effective potential with $\mathbf{x}\equiv(q,\{\mathcal{M}_{\boldsymbol{\alpha}}\})$. It follows from (27) that to find this factor we need to evaluate the Laplace-transformed probability (41) and (43) at

$$\theta = \tfrac{1}{2}\partial s_{\rm ann}/\partial q, \quad y_{\boldsymbol{\alpha}} = \tfrac{1}{2}\partial s_{\rm ann}/\partial \mathcal{M}_{\boldsymbol{\alpha}}. \tag{57}$$

This is where the Lagrange multipliers come in handy as we can immediately claim that

$$\partial s_{\rm ann}/\partial q = -\lambda, \tag{58}$$

$$\partial s_{\rm ann}/\partial \mathcal{M}_{\boldsymbol{\alpha}} = \sum_p \ln \frac{\mathcal{M}_{\boldsymbol{\alpha}}}{\mu^p_{\boldsymbol{\alpha}}} - \ln \mathcal{M}_{\boldsymbol{\alpha}}. \tag{59}$$

Note that in differentiating with respect to $\mathcal{M}_{\boldsymbol{\alpha}}$ above we omitted the constant term. This is permissible since only differences $\partial q_{\rm ann}/\partial \mathcal{M}_{\boldsymbol{\alpha}} - \partial q_{\rm ann}/\partial \mathcal{M}_{\boldsymbol{\alpha}'}$ appear in Eq. (43). A further refinement is to write

$$\sum_p \ln \frac{\mathcal{M}_{\boldsymbol{\alpha}}}{\mu^p_{\boldsymbol{\alpha}}} = \sum_p \ln \frac{1+\sigma_p q}{2} = K \ln \frac{\sqrt{1-q^2}}{2} + \sum_p \sigma_p \tanh^{-1} q. \tag{60}$$

Using this in the Eqs. (27) and (43), we obtain

$$\ell(q,\{\mathcal{M}_{\boldsymbol{\alpha}}\}) = \frac{1}{Z}\sum_{\sigma,\mathbf{k}} \prod_{p,\boldsymbol{\alpha}} \times \left(\mu^p_{\boldsymbol{\alpha}} e^{1/2\Sigma_{p'}(\sigma_{p'}-\sigma'_{p'})\tanh^{-1} q} \sqrt{\frac{\mathcal{M}_{\boldsymbol{\alpha}'}}{\mathcal{M}_{\boldsymbol{\alpha}}}}\right)^{k^p_{\boldsymbol{\alpha}}}/k^p_{\boldsymbol{\alpha}}!. \tag{61}$$

Since $1/2\Sigma_{p'}(\sigma_{p'}-\sigma'_{p'}) \equiv \sigma_p$ (where $\boldsymbol{\alpha}'$ is obtained from $\boldsymbol{\alpha}$ by flipping pth bit) and also

$$\mathcal{M}_{\boldsymbol{\alpha}}/\mu^p_{\boldsymbol{\alpha}} = \frac{\sqrt{1-q^2}}{2} e^{\sigma_p \tanh^{-1} q}, \tag{62}$$

the expression is considerably simplified

$$\ell(q,\{\mathcal{M}_{\boldsymbol{\alpha}}\}) = \frac{2}{Z}\exp\left(\frac{2}{\sqrt{1-q^2}} \sum_{\langle \boldsymbol{\alpha},\boldsymbol{\alpha}'\rangle} \sqrt{\mathcal{M}_{\boldsymbol{\alpha}}\mathcal{M}_{\boldsymbol{\alpha}'}}\right), \tag{63}$$

where the sum is over pairs $\langle \boldsymbol{\alpha}, \boldsymbol{\alpha}'\rangle$ that differ in exactly one position

$$\frac{1}{2}\sum_{p=1}^{K} |\boldsymbol{\alpha}_j - \boldsymbol{\alpha}'_j| = 1. \tag{64}$$

To evaluate Z we write

$$Z = \frac{2}{\sqrt{1-q^2}}\sqrt{e^{\mu_+}e^{\mu_-}} = \frac{2}{\sqrt{1-q^2}}\exp\left(\frac{\mathcal{M}_+}{1+q} + \frac{\mathcal{M}_-}{1-q}\right) \tag{65}$$

and the expression for ℓ becomes

$$\ell(q,\{\mathcal{M}_{\boldsymbol{\alpha}}\}) = \sqrt{1-q^2}\exp\left(\frac{2\Sigma_{\langle \boldsymbol{\alpha},\boldsymbol{\alpha}'\rangle}\sqrt{\mathcal{M}_{\boldsymbol{\alpha}}\mathcal{M}_{\boldsymbol{\alpha}'}}}{\sqrt{1-q^2}} - \frac{\mathcal{M}_+}{1+q} - \frac{\mathcal{M}_-}{1-q}\right). \tag{66}$$

Here $\mathcal{M}_\pm$ are given in (51).

We note that the effective potential $f(q,\{\mathcal{M}_{\boldsymbol{\alpha}}\}) = \varepsilon(\{\mathcal{M}_{\boldsymbol{\alpha}}\}) - \Gamma\ell(q,\{\mathcal{M}_{\boldsymbol{\alpha}}\})$ is symmetric with respect to permutation of individual components in $\{\mathcal{M}_{\boldsymbol{\alpha}}\}$ corresponding to different orders of -1's and $+1$'s in the vectorial index $\boldsymbol{\alpha}$. We look for the minimum of $f(q,\{\mathcal{M}_{\boldsymbol{\alpha}}\})$ using the symmetric ansatz

$$\mathcal{M}_{\boldsymbol{\alpha}} = \binom{K}{m}^{-1} M_m, \quad m = \sum_{p=1}^{K} \frac{1-\alpha_p}{2}, \tag{67}$$

where m is the number of -1's in $\boldsymbol{\alpha}$. Substituting (67) into (66) and rewriting

$$\overline{\ell}(q,\{M_m\}) = \sqrt{1-q^2}\exp\left(\frac{2\Sigma_{m=0}^{K-1}\sqrt{(m+1)(K-m)M_m M_{m+1}}}{\sqrt{1-q^2}} - \frac{K\gamma + q\Sigma_{m=0}^{K}(K-2m)M_m}{1-q^2}\right) \tag{68}$$

where we defined $\overline{\ell}(q,\{M_m\}) \equiv \ell(q,\{\mathcal{M}_{\boldsymbol{\alpha}}\})$. The effective potential is then

$$\overline{f}(q,\{M_m\}) = \varepsilon(\{M_m\}) - \Gamma\overline{\ell}(q,\{M_m\}) \quad (QA), \tag{69}$$

with energy given in (39). In the case of the SA algorithm the corresponding free-energy functional (33) is

$$\overline{f}(q,\{M_m\}) = \varepsilon(\{M_m\}) - T\overline{s}(q,\{M_m\}) \quad (SA), \tag{70}$$

where the entropy function equals

$$\overline{s}(q,\{M_m\}) = -q\tanh^{-1} q + (\gamma K - 1)\ln\frac{\sqrt{1-q^2}}{2} - \left(\sum_{m=0}^{K}(K-2m)M_m\right)\tanh^{-1} q - \sum_{m=0}^{K} M_m \ln\frac{M_m}{\binom{K}{m}}. \tag{71}$$

If we were to use an even smaller set of macroscopic parameters (e.g., only the energy ε) we can still employ formula (68) with the proviso that unspecified variables should be taken to equal their most likely values, i.e., those that maximize the entropy $\overline{s}(q,\{M_m\})$ not the landscape $\overline{\ell}(q,\{\mathcal{M}_m\})$. For example, in the case of energy-only landscapes, $\overline{\ell} = \overline{\ell}(\varepsilon)$, the values $q,\{M_m\}$ that maximize $\overline{s}(q,\{M_m\})$ for a given energy ε and number of hyperedges $\gamma N(\Sigma_{m=0}^{K} M_m \equiv \gamma)$ should be computed and then substituted into the expression for $\overline{\ell}$ (68).

We compute, within the annealing approximation, the point of static transition γ_c (cf. Fig. 1), where the entropy of the macroscopic state with zero energy vanishes, $s(0)=0$, and the dynamic transition γ_d; for connectivities $\gamma > \gamma_d$ an effective potential (69) exhibits a global bifurcation for some $\Gamma = \Gamma_*$. The resulting values are given in Table I (see also Figs. 2 and 3). Note that in 1-in-3 SAT and K-NAE-SAT for ($K=3$, 4, 5) we find no dynamical phase transition before the satisfiability threshold (cf. Fig. 1).

In Fig. 4 we plot time variations of the landscape parameters, $M_m = M_{*m}$, corresponding to the global minimum of the effective potential. In Fig. 5 we plot a time-variation of the

TABLE I. Annealing bounds for dynamic (γ_d) and static γ_c) transition for positive 1-in-K SAT and positive K-NAE SAT for different values of the number of variables in a clause K. No value (—) indicates the absence of dynamical transition.

	K	3	4	5	6	7	8	9	10
1-in-K	γ_d	—	0.650	0.557	0.475	0.416	0.371	0.335	0.305
	γ_c	0.805	0.676	0.609	0.548	0.500	0.461	0.428	0.400
K-NAE	γ_d	—	—	—	19.8	34.9	61.7	109	196
	γ_c	2.41	5.19	10.7	21.8	44.0	88.4	177	355

scaled ground-state energy g given by the value of the effective potential at its minimum. Singular behavior corresponding to the first-order quantum phase transition at certain $\tau = \tau_*(\Gamma = \Gamma_*)$ can be clearly seen from the figures. Plots in Figs. 4 and 5 correspond to precisely the static transition $\gamma = \gamma_c$ for the case of $K=4$ in 1-in-K SAT problem. In the region $\gamma_d < \gamma < \gamma_c$ there are an exponential (in N) number of solutions to the satisfiability problem but the runtime of the quantum adiabatic algorithm to find any of them also scales exponentially with N. This is a *hard* region for this algorithm. We note that in the limit of $K \to \infty$ the annealing approximation becomes exact. Together with the fact that for large K γ_d and γ_c seem to be distinctly different provides evidence that this result (the existence of a hard region for quantum adiabatic algorithm) is robust.

VI. UNIVERSALITY PROPERTY FOR TRANSITION PROBABILITIES

Here we study the universal features of the transition probability in (11) for the set of macroscopic variables corresponding to the (normalized) total Ising spin q and numbers of clauses of different types $\{M_m\}$ (39) (the type of a clause is equal to the number of unit bits involved in the clause). For simplicity, we shall focus in this section on the case $K=3$ only.

To clarify the above choice of macroscopic variables we consider an auxiliary quantity: a conditional probability distribution of the macroscopic variables $(q,\{M_m\})$ over the set of all possible configurations $\boldsymbol{\sigma}$ obtained by flipping r bits of the configuration $\boldsymbol{\sigma}'$. The first moments of this distribution corresponding to M_m,

$$\mu_m = \binom{N}{r}^{-1} \sum_{\boldsymbol{\sigma}} \delta[d(\boldsymbol{\sigma}' - \boldsymbol{\sigma}), r] M_m(\boldsymbol{\sigma}, \mathcal{I}), \quad m = 0, \ldots, K, \tag{72}$$

can be easily computed by counting the number of ways one can flip r bits in configuration $\boldsymbol{\sigma}'$ to transform a K-bit clause of m' type (i.e., with m' unit bits) into a clause of the mth type

$$\mu_m = \binom{N}{r}^{-1} \sum_{p,m'=0}^{K} M_{m'} \binom{m'}{p} \binom{K-m'}{m-m'+p} \times \binom{N-K}{r-2p-m+m'} \tag{73}$$

[here we use the convention $\binom{n}{m} \equiv 0$ for $m<0$ and $m>n$]. In the double sum above, values of $\mathcal{M}_{m'}$ are multiplied by the number of possible ways to flip three groups of bits: p unit bits in a clause of m'-type, $p+m-m'$ zero bits of this clause, and $r-2p-m+m'$ bits of the configuration $\boldsymbol{\sigma}'$ that do not belong to the clause. Similarly, one can show that the first moment corresponding to the variable q equals $q'(1-2r/N)$. It is clear that dependence of the first moments on the ancestor configuration $\boldsymbol{\sigma}'$ is only via the variables q', M'_m for that configuration.

In the limit, $r \gg 1$, the above conditional distribution has a Gaussian form with respect to q and M_m. Elements of the covariance matrix $\Sigma_{mq}^{m'q'}(\boldsymbol{\sigma}') = O(r)$, and correspondingly, the characteristic width of the distribution is $O(r^{1/2})$. For a configuration $\boldsymbol{\sigma}'$ randomly sampled in the box $(q,\{M_m\})$ the

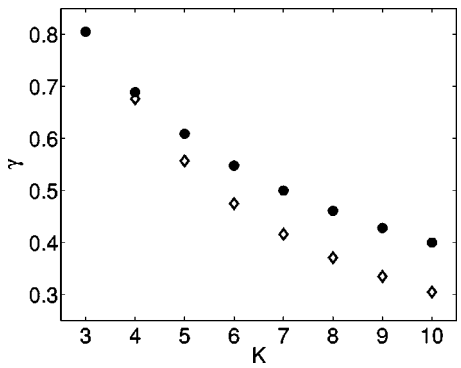

FIG. 2. Static γ_c (circles) and dynamic γ_d (diamonds) transition for positive 1-in-K SAT for various values of K.

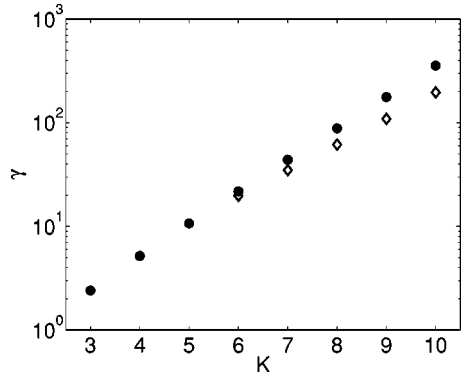

FIG. 3. Static γ_c (circles) and dynamic γ_d (diamonds) transition for positive K-NAE SAT for various values of K.

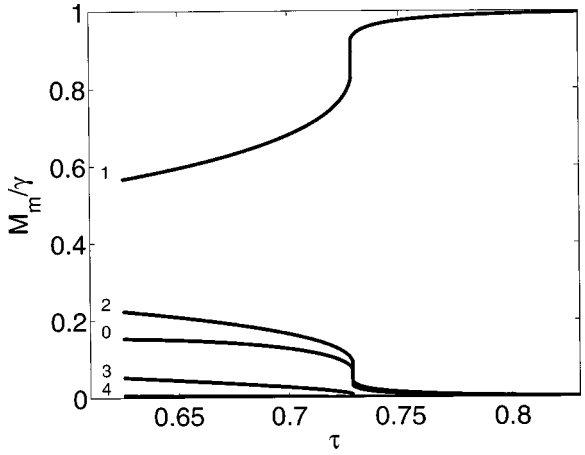

FIG. 4. Plots of the landscape parameters $M_m = M_{*m}$ at the global minimum of the effective potential vs τ for $K=4$ and $\gamma=\gamma_c$ (1-in-K SAT problem). Curves labeled 0–4 correspond to M_{*0}/γ through M_{*4}/γ.

r.m.s. deviation of the elements of $\Sigma_{mq}^{m'q'}(\boldsymbol{\sigma}')$ from their mean values in the box is $O(N^{1/2})$. It is clear that in the limit $r \gg N^{1/2}$ the covariance matrix elements can be replaced by their mean values for the macroscopic state $(q,\{M_m\})$. Therefore in this limit the conditional distribution after r spin flips starting from some macroscopic state depends only on the values of $(q,\{M_m\})$ in this state (universality property).

One can show that for $r \ll N^{1/2}$ the conditional distribution after r spin flips can be expressed via the distribution (11) with $r=1$, using a standard convolution rule. Implicit in our derivation of landscapes is the relation between $r=1$ landscapes and a set of quantities $\{c_{\sigma,\mathbf{k}}\}$. Universality of landscapes should be interpreted as the fact that $\{c_{\sigma,\mathbf{k}}\}$ are self-averaging. Had we included only the energy instead of a full set of parameters, we would not have expected to see such self-averaging in the so-called replica-symmetry-broken phase. It is possible that inclusion of the full set of landscape parameters assures universality. We performed a series of numerical studies to test this hypothesis. In Fig. 6 we present the results of numerical simulations and the comparison with analytic results within the annealing approximation. One can see that the property of self-averaging holds and that even the annealing approximation provides a very good description.

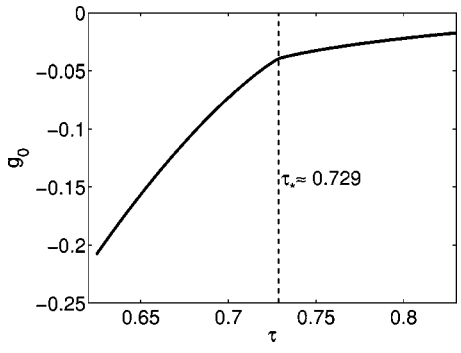

FIG. 5. Scaled energy of adiabatic ground state g_0 vs τ for $K=4$ and $\gamma=\gamma_c$ (1-in-K SAT problem).

VII. RANDOM GRAPH ENSEMBLES WITH REDUCED FLUCTUATIONS

One can easily point to a major deficiency of the annealing approximation—the fact that it fails to correctly predict the satisfiability transition. While part of this can be attributed to the fact that real entropy is slightly different from what is predicted by the annealing approximation, the major source of error is the incorrect assumption that the entropy vanishes at the satisfiability transition. That the entropy does not vanish can be easily seen by examining the structure of the random graph. At any finite connectivity (above percolation) it consists of one giant component and a large $O(N)$ number of small $O(1)$ components. Each small component makes an $O(1)$ contribution to the entropy for a total $O(N)$ contribution, hence the entropy is in fact positive at all connectivities, including the satisfiability threshold.

A. Concept of a core

An improvement over the annealing bound for the satisfiability threshold is possible. Note that clauses outside of the giant component do not affect satisfiability and hence can be disregarded. Similarly, one can identify *irrelevant* clauses and remove them. Irrelevant clauses are those that can be eliminated without changing the satisfiability of the entire problem. We shall illustrate the identification of irrelevant clauses based on local properties for positive K-NAE SAT and positive 1-in-K SAT.

1. Positive K-NAE SAT

For K-NAE SAT we can identify variables that do not enter any clause and remove them without affecting the satisfiability of the formula. Any variable that appears in *exactly one* clause can also be eliminated together with that clause, since the value of that variable can be adjusted to satisfy that clause. As one removes such a clause, other variables may become candidates for removal. One can write an algorithm that iteratively removes variables that appear in zero or exactly one clause until no such variables remain (see Fig. 7). In fact using such an algorithm improves the running time of classical algorithms. The cost of this additional preprocessing is negligible: by using special data structures this algorithm can be made to run in $O(N \ln N)$ time.

It is not surprising that the result of running such a *trimming* algorithm is a set of clauses and variables with a condition that every variable appears in at least two clauses. However, the statistical properties of the remaining *core* are not immediately apparent. As a first step, observe that the resulting core is independent of the order in which clauses and variables were removed. Hence we can study one specific algorithm.

First, we eliminate all variables of degree 0 (that appear in no clauses). In the initial problem all instances with N variables and M clauses were equally probable. The number of vertices of degree 0, N_0 does fluctuate, but for *every specific* value of N_0 all instances with $N-N_0$ variables, and M clauses, and the additional property that each variable appears in at least one clause, are equiprobable. This property

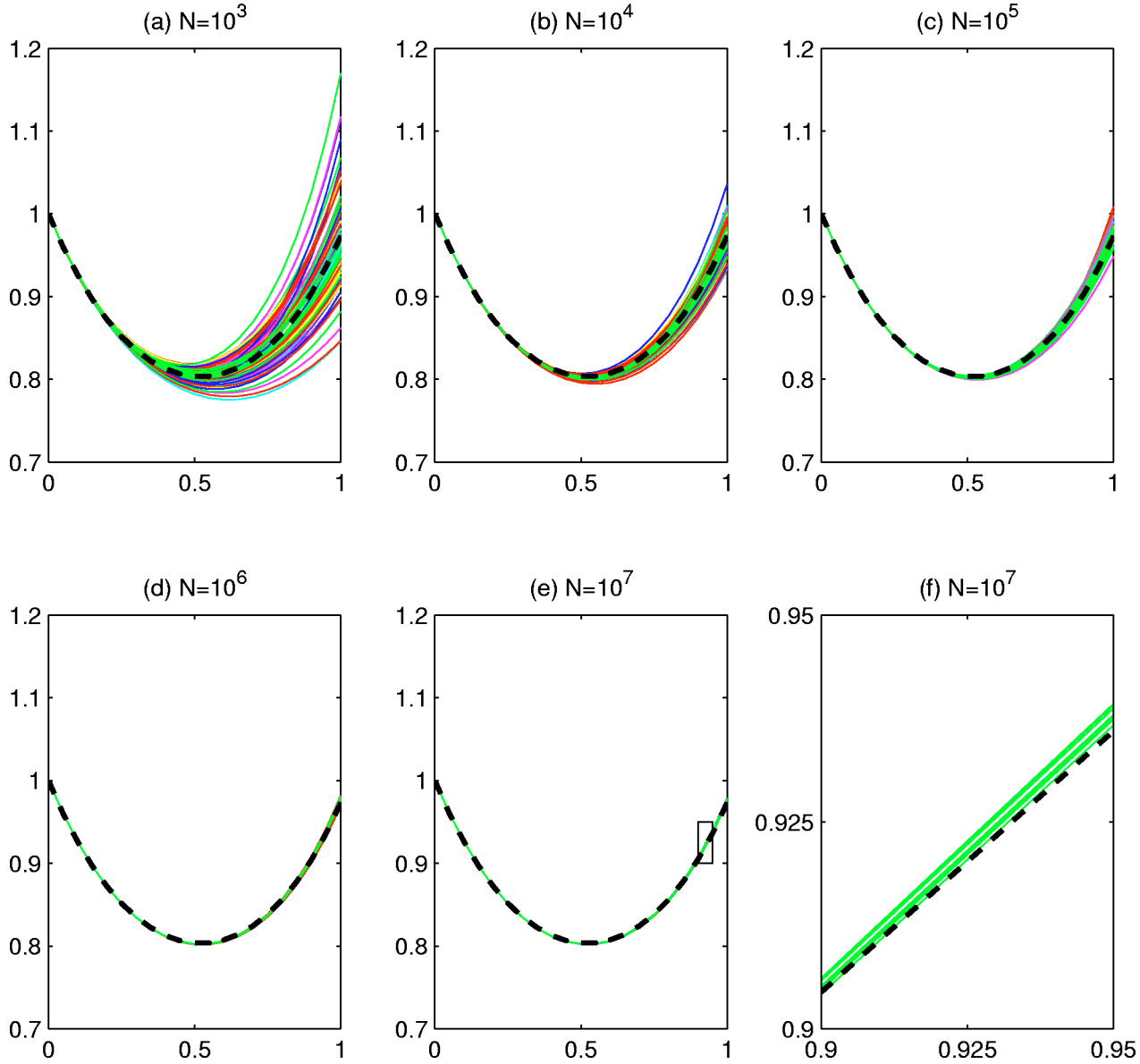

FIG. 6. (Color) Results of numerical simulations and their comparison with theory. Depicted are Laplace transforms of $\mathcal{M}_1$ for 1-in-3 SAT. Numerical results: curves that have different colors correspond to different random problem instances; curves of same color correspond to different random bit strings. The dashed black line is a theoretical result based on the annealing approximation. The insets (a)–(e) depict instances with 10^3, 10^4, 10^5, 10^6, and 10^7 binary variables. Since the error is not visible we replot in (f) a magnified section of inset (e). The bit strings were sampled with $q=0.422$, $M_0=0.048$, $M_1=0.416$, $M_2=0.123$, $M_3=0.013$, corresponding to $M/N=0.6$. These values correspond to the energy $E_\infty/2$ and they are shifted by 10% from the most likely values of $q,\{M_m\}$ for this energy (this shift is $\gg N^{1/2}$). We also note that for 1-in-3 SAT numerical simulations give the static phase transition at $\gamma_c \approx 0.63$.

is referred to as *uniform randomness*. As a next step, identify variables of degree 1 (appearing in exactly one clause). Although their number N_1 also fluctuates, for any fixed N_1, N and M all instances with N variables of which N_1 variables have degree 1 and M clauses are equiprobable.

At each subsequent step of the algorithm we choose *at random* a variable of degree 1 among N_1 candidates, and delete it together with the clause in which it appears. If the degree of any other variable in that clause becomes 0, it is also deleted. Some variables which had degree 2 previously may become degree 1 variables. Obviously $M'=M-1$, but the values of N' and N_1' cannot be predicted. But since the variable chosen for deletion was chosen at random (among all degree 1 variables), one can show that although the values of N' and N_1' cannot be predicted, for every fixed set of $\{N',N_1',M'\}$ all instances are equiprobable.

At the end of the algorithm $N_1 \equiv 0$, hence for fixed N', M', all instances with N' variables, M' clauses and the condition that each variable appear in at least two clauses are equiprobable. Since average changes in N, N_1 and M at each step were $O(1)$ and corresponding deviations were also $O(1)$, after $O(N)$ steps needed for completion of the algorithm, fluctuations in resulting N' and M' are only $O(\sqrt{N})$ by the central limit theorem and can be neglected in our analysis.

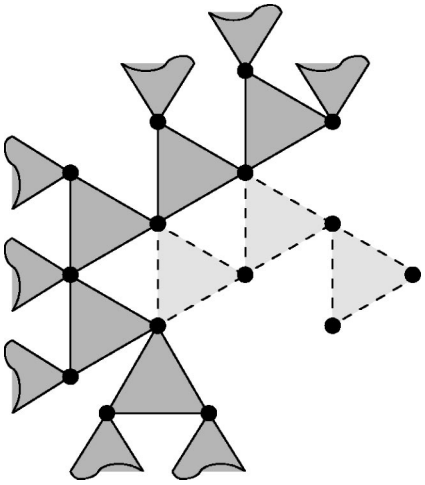

FIG. 7. Example of trimming algorithm for 3-NAE SAT. Variables are represented graphically as vertices and clauses are represented as triangles. Incomplete triangles represent connections to the remainder of the graph (not shown). Shaded clauses are removed by the trimming algorithm.

There are several methods to derive the average resulting values of N', M'. The most straightforward is to study the evolution of N, N_1 and M by solving differential equations for their average values. This is somewhat tedious and less general. We instead resort to a different method of self-consistency equations. For every instance one can identify a set $\mathcal{C}$ of variables that form a *core*, i.e., those that will not be deleted by the trimming algorithm. We now extend that set to $\mathcal{C}'$ using the following rules:

(1) If a variable belongs to $\mathcal{C}$, it also belongs to $\mathcal{C}'$.

(2) If $K-1$ variables in some clause belong to $\mathcal{C}'$, then the remaining variable must also belong to $\mathcal{C}'$.

The minimal set $\mathcal{C}'$ is obtained from $\mathcal{C}$ by iteratively adding variables according to these rules. Let the number of variables in set $\mathcal{C}'$ be equal to qN with $q<1$. Fluctuations in q are $O(1/\sqrt{N})$ and, consequently, are neglected.

Now introduce the $(N+1)$st variable and compare systems with N variables and $N+1$ variables. Together with $(N+1)$st variable introduce ΔM clauses each involving that variable and $(K-1)$ random variables. The number ΔM is a Poisson random variable with parameter $K\gamma$. We can compute the probability that the new variable belongs to $\mathcal{C}'$ of the enlarged instance. The new variable belongs to $\mathcal{C}'$ if for at least one of the ΔM clauses, $K-1$ variables other than the new variables are not in $\mathcal{C}'$ at the same time. Since these clauses are connected to random vertices, that probability can be expressed via q alone and, owing to the fact that ΔM is Poisson, equals $1-\exp(-K\gamma q^{K-1})$. Self-consistency requires that this probability be equal to q:

$$1 - q = e^{-K\gamma q^{K-1}}. \tag{74}$$

For practical purposes we must seek the largest solution to this equation.

Note that the new variable belongs to the core (set $\mathcal{C}$) if not for one, but for *at least two* of ΔM clauses, $K-1$ variables other than the new one are in $\mathcal{C}'$. The probability of that

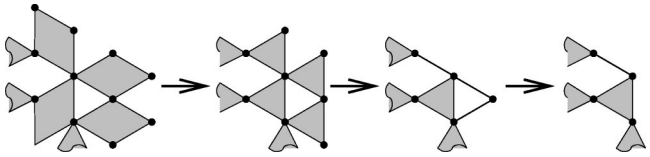

FIG. 8. Example of trimming algorithm for 1-in-4 SAT. Variables are represented graphically as vertices and 4-, 3-, and 2-clauses are represented as rhombi, triangles and edges correspondingly. Incomplete polygons represent connections to the remainder of the graph. The figure depicts evolution of part of the graph under the trimming algorithm.

$$p = 1 - e^{-K\gamma q^{K-1}} - K\gamma q^{K-1} e^{-K\gamma q^{K-1}} \equiv q - K\gamma q^{K-1}(1-q) \tag{75}$$

is equal to the average value of N'/N, and the average connectivity of the new vertex (under the condition that it is in $\mathcal{C}$) enables one to compute M'/N':

$$M'/N' = \frac{1}{K}\frac{K\gamma q^{K-1}(1-e^{-K\gamma q^{K-1}})}{1-(1+K\gamma q^{K-1})e^{-K\gamma q^{K-1}}} \equiv \frac{\gamma q^K}{p} \tag{76}$$

[better expressed as $M'/N = 1/KK\gamma q^{K-1}(1-e^{-K\gamma q^{K-1}}) \equiv \gamma q^K$].

We must mention that the core for K-NAE SAT is in fact identical to that for K-XOR SAT. The latter has been analyzed by a different method [27].

2. Positive 1-in-K SAT

The situation is slightly more interesting in case of positive 1-in-K SAT. Setting a variable that appears in only one clause does not guarantee that the clause will be satisfied, hence the clause cannot be eliminated. Although it cannot be eliminated, it can still be simplified by eliminating the variable. The remaining instance will contain not only K-clauses but also one $(K-1)$-clause. The allowed combinations of variables for $(K-1)$-clauses should be those that have sum of variables equal to *either* 0 *or* 1. In that case the value of the deleted variable can always be adjusted so that the sum of variables in K-clause is exactly 1.

Similarly, at some point $(K-1)$-clauses can be converted to $(K-2)$-clauses, $(K-3)$-clauses, down to 2-clauses. In each case the allowed combinations shall have sum of spins either 0 or 1. Finally, if one can identify a variable that appears in 2-clauses exclusively, this variable can be eliminated together with corresponding 2-clauses, since setting it to 0 shall satisfy all these clauses. As an illustration, see Fig. 8 which depicts $K=4$.

Once again, one can write a trimming algorithm that eliminates such variables and clauses. As before, one can show that all remaining instances must have the property that each variable appear in at least two clauses of any length and at least one clause of length greater than two; and that for fixed number of vertices N', number of 2-clauses $M'_2, \ldots, (K-1)$-clauses M'_{K-1}, K-clauses M'_K, all such instances are equiprobable.

Without going into details (available in our upcoming paper [28]), we should mention that the equations now involve two variables q and q', owing to the separate treatment af-

forded to 2-clauses and clauses of length greater than 2. The self-consistency equations are

$$1-q' = e^{-K\gamma[1-(1-q)^{K-1}-(K-1)q(1-q)^{K-2}]}, \tag{77}$$

$$1-q = (1-q')e^{-K(K-1)\gamma q'(1-q)^{K-2}}, \tag{78}$$

with implicit understanding that the largest solutions q, q' are sought.

The expected values of N' as well as M'_k are given by

$$N'/N = q' - K\gamma[1-(1-q)^{K-1}-(K-1)q(1-q)^{K-2}](1-q), \tag{79}$$

$$M'_2/N = \binom{K}{2}\gamma q'^2(1-q)^{K-2}, \tag{80}$$

$$M'_k/N = \binom{K}{k}\gamma q^k(1-q)^{K-k} \text{ for } k \geqslant 3. \tag{81}$$

Note that results for the core for positive K-NAE SAT and positive 1-in-K SAT allow for a compact formulation through introduction of the *generating function* of the allowed variable degrees.

For the case of K-NAE SAT it is $G(\mu)=\Sigma_{d\geqslant 2}\mu^d/d!=e^\mu-1-\mu$, since degrees of all variables are at least 2. In terms of this $G(\mu)$, equations can be written as

$$N'/N = e^{-\mu}G(\mu), \tag{82}$$

$$M'/N = \frac{1}{K}\mu e^{-\mu}G'(\mu) \tag{83}$$

with $\mu=K\gamma q^{K-1}$, and the equation on q is

$$q = e^{-\mu}G'(\mu). \tag{84}$$

For the case of 1-in-K SAT, G is a function of $(K-1)$ variables reflecting the fact that the degree of each vertex is a vector $(d_2,\ldots,d_K)$ where d_k counts the number of appearances of said variable in k-clauses. The generating function for the remaining core is

$$G(\mu_2,\mu_3,\ldots,\mu_K) = \exp\Big(\sum_{i=2}^K \mu_i\Big) - e^{\mu_2} - \sum_{i=3}^K \mu_i. \tag{85}$$

There appears a set $\{q_2,\ldots,q_K\}$ such that $q_k=(\partial/\partial\mu_k)G(\{\mu_i\})$. Obviously, $q_3=q_4=\cdots=q_K$. Setting

$$\mu_2 = 2\binom{K}{2}\gamma q'(1-q)^{K-2}, \tag{86}$$

$$\mu_k = k\binom{K}{k}\gamma q^{k-1}(1-q)^{K-k} \text{ for } k \geqslant 3, \tag{87}$$

N' and M'_k can be compactly written as

$$N'/N = \exp\Big(-\sum_{i=2}^K \mu_i\Big)G(\{\mu_i\}), \tag{88}$$

$$M'_k/N = \frac{1}{k}\mu_k \exp\Big(-\sum_{i=2}^K \mu_i\Big)\frac{\partial}{\partial\mu_k}G(\{\mu_i\}). \tag{89}$$

B. Improved annealing bound

Once irrelevant clauses have been removed we expect the entropy at the satisfiability transition to be much closer to zero. We have already made predictions for the number of remaining variables and clauses after application of the trimming algorithm starting from a random graph of connectivity γ. We can compute the entropy of the remaining core. Using the critical connectivity at which the annealed entropy of the core alone becomes 0 as an estimate of the satisfiability transition is an improvement over the traditional annealing approximation. We are motivated by two contributing factors: (i) the rigorous mathematical proof that the disorder is relevant for the satisfiability transition relies on the presence of irrelevant clauses, hence their removal can sometimes make disorder irrelevant, and (ii) applied to K-XOR SAT, this improved bound becomes *exact* [27].

Doing the annealing approximation on a core is hampered by the fact that clauses can no longer be assumed uncorrelated. However, the technique we introduced in this paper is well-suited for this example. The annealed entropy equals

$$s_{\rm ann} = \frac{1}{N'}\ln\mathcal{N}_{S,G} - \frac{1}{N'}\ln N_{\mathcal{G}}, \tag{90}$$

where $\mathcal{N}_{\mathcal{G}}$ counts the number of possible disorders and $\mathcal{N}_{S,\mathcal{G}}$ is the total number of allowed spin-disorder configurations. We now separately consider K-NAE SAT and 1-in-K SAT.

1. Positive K-NAE SAT

Consider the number of possible disorder realizations with N' variables, M' clauses, with the constraint that each variable appear in at least two clauses. Each variable can be characterized by the vector $\mathbf{k}$ with K components, each component k_p counting the number of clauses where said variable appears in the pth position. Treating disorders that differ by permuting different clauses or permuting variables within a clause as different and fixing the fractions of vertices with a particular realization of $\mathbf{k}$ to $c_{\mathbf{k}}$, the normalized logarithm of the count of possible disorders is

$$\frac{1}{N'}\ln\mathcal{N}_{S,\mathcal{G}} \equiv s'_0[N',M';\{c_{\mathbf{k}}\}] = -\sum_{\mathbf{k}} c_{\mathbf{k}}\ln\Big[c_{\mathbf{k}}\prod_p k_p!\Big] + K\frac{M'}{N'}\ln M'. \tag{91}$$

We must maximize this expression with respect to $c_{\mathbf{k}}$ subject to the constraints

$$\sum_{\mathbf{k}} k_p c_{\mathbf{k}} = M'/N' \tag{92}$$

and that $c_{\mathbf{k}}=0$ for $\Sigma_p k_p<2$.

Introducing Lagrange multipliers μ_p, the expression for $c_{\mathbf{k}}$ becomes

$$c_{\mathbf{k}} = \frac{1}{G(\Sigma_p\mu_p)}\prod_p \frac{\mu_p^{k_p}}{k_p!}. \tag{93}$$

Echoing the constraint that $\Sigma_p k_p\geqslant 2$, the normalization factor is $G(\Sigma_p\mu_p)$ where $G(x)=e^x-1-x$—the familiar generating

function of the core. Using the dual transformation we can rewrite the entropy as

$$s_0'[N',M'] = \min_{\mu_p}\left\{\sum_p (M'/N')\ln\frac{M'/N'}{\mu_p} + \ln G\left(\sum_p \mu_p\right)\right\} + \frac{KM'}{N'}\ln N'. \tag{94}$$

Comparing this expression with Eqs. (82) and (83) we observe that the minimum is achieved for $\mu_p=(1/K)\mu \equiv \gamma q^{K-1}$, γ being the connectivity of untrimmed random graph.

Now we proceed to count all possible combinations of spin assignments and disorder realizations $\mathcal{N}_{S,\mathcal{G}}$. Corresponding entropy is in general a function of $\{\mathcal{M}'_{\boldsymbol{\alpha}}\}$ where $\mathcal{M}'_{\boldsymbol{\alpha}}$ is the number of clauses with variables having values described by a vector $\{\boldsymbol{\alpha}_p\}\equiv\boldsymbol{\alpha}$, divided by N' so that $\Sigma_{\boldsymbol{\alpha}}\mathcal{M}'_{\boldsymbol{\alpha}}=M'/N'$. In complete analogy with results of Sec. V A we obtain

$$s_1'[N',M';\{\mathcal{M}'_{\boldsymbol{\alpha}}\};\{c_{\sigma,\mathbf{k}}\}] = -\sum_{\sigma,\mathbf{k}} c_{\sigma,\mathbf{k}}\ln\left[c_{\sigma,\mathbf{k}}\prod_{p,\boldsymbol{\alpha}} k^p_{\boldsymbol{\alpha}}!\right] + (K-1)\sum_{\boldsymbol{\alpha}}\mathcal{M}'_{\boldsymbol{\alpha}}\ln\mathcal{M}'_{\boldsymbol{\alpha}} + \frac{M'}{N'}\ln\frac{M'}{N'} + \frac{KM'}{N'}\ln N'. \tag{95}$$

Optimizing this with respect to $c_{\sigma,\mathbf{k}}$ subject to familiar constraints

$$\sum_{\sigma,\mathbf{k}} k^p_{\boldsymbol{\alpha}} c_{\sigma,\mathbf{k}} = \mathcal{M}_{\boldsymbol{\alpha}} \tag{96}$$

and the constraint that $c_{\sigma,\mathbf{k}}=0$ if $\Sigma_{p,\boldsymbol{\alpha}}k^p_{\boldsymbol{\alpha}}<2$, the expression can be equivalently rewritten as

$$s_1'[N',M';\{\mathcal{M}'_{\boldsymbol{\alpha}}\}] = \min_{\mu^p_{\boldsymbol{\alpha}}}\left\{\sum_{p,\boldsymbol{\alpha}}\mathcal{M}'_{\boldsymbol{\alpha}}\ln\frac{\mathcal{M}'_{\boldsymbol{\alpha}}}{\mu^p_{\boldsymbol{\alpha}}} + \ln Z[\{\mu^p_{\boldsymbol{\alpha}}\}]\right\} + \frac{M'}{N'}\ln\frac{M'}{N'} - \sum_{\boldsymbol{\alpha}}\mathcal{M}'_{\boldsymbol{\alpha}}\ln\mathcal{M}'_{\boldsymbol{\alpha}} + \frac{KM'}{N'}\ln N', \tag{97}$$

with $Z[\{\mu^p_{\boldsymbol{\alpha}}\}]$ given instead by

$$Z[\{\mu^p_{\boldsymbol{\alpha}}\}] = G\left(\sum_{p,\boldsymbol{\alpha}}\delta[\boldsymbol{\alpha}_p;1]\mu^p_{\boldsymbol{\alpha}}\right) + G\left(\sum_{p,\boldsymbol{\alpha}}\delta[\boldsymbol{\alpha}_p;-1]\mu^p_{\boldsymbol{\alpha}}\right). \tag{98}$$

Labeling arguments by μ_+ and μ_-, respectively, allows us to simplify this to

$$s_1'[\{\mathcal{M}'_{\boldsymbol{\alpha}}\}] = \min_{\mu_\pm}\left\{\mathcal{M}'_+\ln\frac{\mathcal{M}'_+}{\mu_+} + \mathcal{M}'_-\ln\frac{\mathcal{M}'_-}{\mu_-} + \ln[G(\mu_+) + G(\mu_-)]\right\} + \frac{M'}{N'}\ln\frac{M'}{N'} - \sum_{\boldsymbol{\alpha}}\mathcal{M}'_{\boldsymbol{\alpha}}\ln\mathcal{M}'_{\boldsymbol{\alpha}} + \frac{KM'}{N'}\ln N' \tag{99}$$

with $\mathcal{M}'_+=\Sigma_{\boldsymbol{\alpha}}(\Sigma_p\delta[\boldsymbol{\alpha}_p;1])\mathcal{M}'_{\boldsymbol{\alpha}}$ and $\mathcal{M}'_-=\Sigma_{\boldsymbol{\alpha}}(\Sigma_p\delta[\boldsymbol{\alpha}_p;-1])\mathcal{M}'_{\boldsymbol{\alpha}}$.

The correct annealed entropy is given by the difference of these expressions

$$s'_{\mathrm{ann}}[N',M';\{\mathcal{M}'_{\boldsymbol{\alpha}}\}] = s_1'[N',M';\{\mathcal{M}'_{\boldsymbol{\alpha}}\}] - s_0'[N',M']. \tag{100}$$

This enables us to find the improved bound on the satisfiability threshold (where $H_{\mathrm{ann}}=0$) or to compute the most likely values of $\{\mathcal{M}'_{\boldsymbol{\alpha}}\}$ for a particular energy E.

Note that for positive K-NAE SAT corrections to the static threshold due to this improved approximation are minute, since the transition happens at large connectivities, where the simple annealing approximation adequately describes the transition.

2. Positive 1-in-K SAT

For 1-in-K SAT the derivation is quite similar. An important addition is that the clauses can have any length from 2 to K, hence index $\mathbf{k}$ should reflect that fact. Since the calculations are similar in spirit, we shall only provide the results

$$s_0'[N',\{M'_k\}] = \min_{\mu_k}\left\{k\frac{M'_k}{N'}\ln\frac{kM'_k/N'}{\mu_k} + \ln G(\{\mu_k\})\right\} + \sum_{k=2}^{K}\frac{kM'_k}{N'}\ln N', \tag{101}$$

with $G(\{\mu_k\})=\exp(\Sigma_{k=2}^K\mu_k)-e^{\mu_k}-\Sigma_{k=3}^K\mu_k$, and

$$s_1' = \min_{\mu_{k,\pm}}\left\{\sum_{k=2}^{K}\left(\mathcal{M}'_{k,+}\ln\frac{\mathcal{M}'_{k,+}}{\mu_{k,+}} + \mathcal{M}'_{k,-}\ln\frac{\mathcal{M}'_{k,-}}{\mu_{k,-}}\right) + \ln[G(\{\mu_{k,+}\}) + G(\{\mu_{k,-}\})]\right\} + \sum_{k=2}^{K}\left[\mathcal{M}'_k\ln\mathcal{M}'_k - \sum_{\boldsymbol{\alpha}}\mathcal{M}'_{k,\boldsymbol{\alpha}}\ln\mathcal{M}'_{k,\boldsymbol{\alpha}}\right] + \sum_{k=2}^{K}\frac{kM'_k}{N'}\ln N', \tag{102}$$

and the complete expression for the annealed entropy is

$$s'_{\mathrm{ann}}[N',\{\mathcal{M}'_k\};\{\mathcal{M}'_{k,\boldsymbol{\alpha}}\}] = s_1'[\{\mathcal{M}'_{k,\boldsymbol{\alpha}}\}] - s_0'[N',\{M'_k\}]. \tag{103}$$

The numerical predictions for the point where the entropy becomes zero are provided in Table II.

TABLE II. Dynamic and static transition for positive 1-in-K SAT with the improved annealing approximation and with the old method using $\{M_m\}$ as landscape parameters. The prediction of γ_c' for $K=3$ compares favorably with the result of simulations of $\gamma_c' \approx 0.63$. No value (—) indicates the absence of a dynamical transition.

	K	3	4	5	6	7	8	9	10
Improved	γ_d'	—	—	0.535	0.469	0.421	0.379	0.344	0.317
	γ_c	0.653	0.609	0.553	0.507	0.468	0.435	0.407	0.382
Old	γ_d	—	0.671	0.552	0.471	0.413	0.368	0.333	0.304
	γ_c	0.805	0.676	0.609	0.548	0.500	0.461	0.428	0.400

VIII. QAA ALOGORITHM ON A CORE: EXTENDED LANDSCAPES

Once we have reexpressed the entropy on a reduced graph, it is only natural to implement the quantum adiabatic evolution directly on the reduced graph. Correspondingly, we shall need to recompute the landscapes for the reduced graph.

A. Positive K-NAE SAT

This case entails the least difficulty, since we can use the same landscape parameters $\{\mathcal{M}'_{\boldsymbol{\alpha}}\}$, the difference being the exclusion of the total spin from the list of parameters. The central quantity—$\ell'(\{\mathcal{M}'_{\boldsymbol{\alpha}}\})$—is still expressed in a similar form:

$$\ell'(\{\mathcal{M}'_{\boldsymbol{\alpha}}\}) = \sum_{\sigma,\mathbf{k}} c_{\sigma,\mathbf{k}} \exp\left[\frac{1}{2}\sum_{p,\boldsymbol{\alpha}} k^p_{\boldsymbol{\alpha}}\left(\frac{\partial s'_{\mathrm{ann}}}{\partial \mathcal{M}'_{\boldsymbol{\alpha}}} - \frac{\partial s'_{\mathrm{ann}}}{\partial \mathcal{M}'_{\overline{\boldsymbol{\alpha}}(p,\boldsymbol{\alpha})}}\right)\right]. \tag{104}$$

Notably, the sum over $\mathbf{k}$ is now restricted to $|\mathbf{k}| \geqslant 2$. The derivatives of the entropy are still

$$\frac{\partial s'_{\mathrm{ann}}}{\partial \mathcal{M}'_{\boldsymbol{\alpha}}} = \sum_p \ln \frac{\mathcal{M}'_{\boldsymbol{\alpha}}}{\mu^p_{\boldsymbol{\alpha}}} - \ln \mathcal{M}'_{\boldsymbol{\alpha}}. \tag{105}$$

For $\boldsymbol{\alpha}$, $\boldsymbol{\alpha}'$ differing in exactly one position, we shall have

$$\frac{1}{2}\left(\frac{\partial s'_{\mathrm{ann}}}{\partial \mathcal{M}'_{\boldsymbol{\alpha}}} - \frac{\partial s'_{\mathrm{ann}}}{\partial \mathcal{M}'_{\boldsymbol{\alpha}'}}\right) = \frac{1}{2}\ln \frac{\mu^p_{\boldsymbol{\alpha}'}}{\mu^p_{\boldsymbol{\alpha}}}. \tag{106}$$

Next, using $c_{\sigma,\mathbf{k}} = (1/Z)(\mu^p_{\boldsymbol{\alpha}})^{k^p_\alpha}/k^p_{\boldsymbol{\alpha}}!$, for $|\mathbf{k}| \geqslant 2$ and Eq. (43), we are able to write, in terms of generating function $G(\mu)$:

$$\ell'(\{\mathcal{M}'_{\boldsymbol{\alpha}}\}) = \frac{2}{Z} G\left(\sum_{\langle \boldsymbol{\alpha},\boldsymbol{\alpha}'\rangle} \sqrt{\mu^p_{\boldsymbol{\alpha}}\mu^p_{\boldsymbol{\alpha}'}}\right). \tag{107}$$

Substituting $\mathcal{M}'_{\boldsymbol{\alpha}}/\mu^p_{\boldsymbol{\alpha}} = \mathcal{M}'_{\boldsymbol{\alpha}_p}/\mu_{\boldsymbol{\alpha}_p}$, we can rewrite this as

$$\ell'(\{\mathcal{M}'_{\boldsymbol{\alpha}}\}) = \frac{2}{G(\mu_+) + G(\mu_-)} \times G\left(\sqrt{\frac{\mu_+\mu_-}{\mathcal{M}'_+\mathcal{M}'_-}} \sum_{\langle \boldsymbol{\alpha},\boldsymbol{\alpha}'\rangle} \sqrt{\mathcal{M}'_{\boldsymbol{\alpha}}\mathcal{M}'_{\boldsymbol{\alpha}'}}\right). \tag{108}$$

Note that for the landscapes on the original graph without the spin variable, this expression is valid with $G(\mu)$ redefined to be $G(\mu) = e^\mu$.

B. Positive 1-in-K SAT

The notion of landscape parameters has to be generalized, since clauses of any length can appear. Correspondingly, we choose a set $\{\mathcal{M}'_{k,\boldsymbol{\alpha}}\}$ to serve as landscape parameters. In contrast to K-NAE SAT, we have a total of $\Sigma_{k=2}^K (k+1) = (K-1)(K-2)/2$ parameters (with symmetries of $\mathcal{M}'_{k,\boldsymbol{\alpha}}$ taken into account).

The derivation of landscapes can be generalized to include several types of clauses. The final answer is itself a generalization of Eq. (66)

$$\ell'(\{\mathcal{M}'_{k,\boldsymbol{\alpha}}\}) = \frac{2}{G(\{\mu_{k,+}\}) + G(\{\mu_{k,-}\})} \times G\left(\left\{\sqrt{\frac{\mu_{k,+}\mu_{k,-}}{\mathcal{M}_{k,+}\mathcal{M}_{k,-}}} \sum_{\langle \boldsymbol{\alpha},\boldsymbol{\alpha}'\rangle} \sqrt{\mathcal{M}'_{k,\boldsymbol{\alpha}}\mathcal{M}'_{k,\boldsymbol{\alpha}'}}\right\}\right). \tag{109}$$

As before $G(\{\mu_k\}) = \exp(\Sigma_{i=2}^K \mu i) - e^{\mu_2} - \Sigma_{i=3}^K \mu_i$.

We can exploit the symmetry of $\mathcal{M}'_{k,\boldsymbol{\alpha}}$ to write

$$\sum_{\langle \boldsymbol{\alpha},\boldsymbol{\alpha}'\rangle} \sqrt{\mathcal{M}'_{k,\boldsymbol{\alpha}}\mathcal{M}'_{k,\boldsymbol{\alpha}'}} = \sum_{m=0}^{k-1} \sqrt{(m+1)(k-m)M'_{k,m}\mathcal{M}'_{k,m+1}}. \tag{110}$$

The same is possible for K-NAE SAT; in fact it is precisely this form that is used in numerical calculations.

C. Numerical results

Here we provide the numerical results for the satisfiability transition as determined by maximizing the entropy for energy $E=0$ and solving $s'_{\mathrm{ann}}=0$. And we also list the location of the dynamical transition, indicated by the global bifurcation in $f' = \varepsilon' - \Gamma\ell'$. All results are expressed in terms of the connectivity of the original random graph for easy comparison with Table I.

We observed that this refinement of our analysis leaves γ_d and γ_c of K-NAE SAT essentially unchanged. This is the manifestation of the fact that if either K or γ is large, then the core is not much different from the original graph (i.e., that $q \approx 1$). In contrast, the difference for 1-in-K SAT is quite

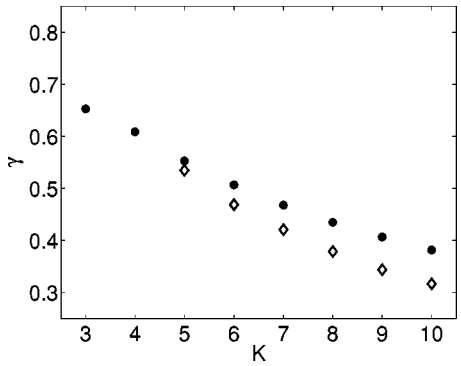

FIG. 9. Static (circles) and dynamic (diamonds) transition for various values of K for positive 1-in-K SAT.

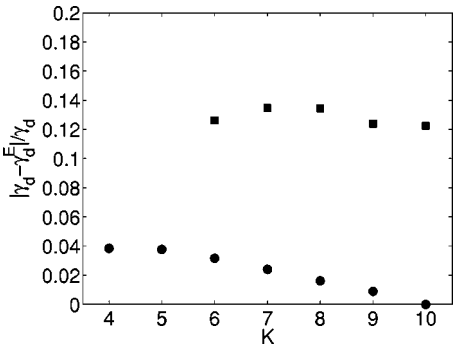

FIG. 10. Relative difference between the predictions for the dynamical phase transition point in the case of full (γ_d) and energy-only (γ_d^E) landscapes vs of K for 1-in-K SAT (circles) and K-NAE SAT (squares).

noticable. For consistency, we compare the location of the dynamic phase transition computed on the core to that computed on the original graph using only M_m as landscape parameters (omitting total spin, as it is not among the parameters for computations performed on a core). We also include new, better, bounds on the static transition. All results are summarized in Table II and Fig. 9.

IX. CONCLUSION

We have formulated an ansatz of landscapes and studied the complexity of the quantum adiabatic algorithm within the annealing approximation and found the existence of a dynamic transition and a hard (exponential) region above that dynamic transition. However, a similar analysis of simulated annealing did not reveal any phase transitions. We explain this as follows. The annealing approximation should fail for sufficiently small energies. It is commonly known that simulated annealing can find suboptimal solutions with very small energies very efficiently, but it takes an exponentially long time to actually reach the ground state. The annealing approximation does not correctly describe very small energies and cannot be used to establish its complexity. Note that we can reconcile this with the fact that the annealing approximation becomes *exact* in the limit when the number of bits in a clause $K\to\infty$: if the annealing approximation fails for some $E\lesssim E_K$ we expect that E_K is decreasing to zero as K increases. However for any finite K, the free energy computed within the annealing approximation is free from any singularities indicative of a phase transition. To study the complexity of simulated annealing one needs to use the tools of spin glass theory, in particular, the replica trick [25,26,29] (see also below).

In contrast, in our analysis of the quantum adiabatic algorithm, we observed a first-order phase transition, and, importantly, it happens for energies $E_*=O(E_\infty)$ [where E_∞ is the expected energy at infinite temperature, $E_\infty=(1/2^n)\Sigma_z E_z$]. Moreover, the energies on both sides of the transition, relative to E_∞ seem not to change appreciably with increasing K. Since the annealing approximation for this range of energies can be used, the prediction for the dynamic transition should survive, though the exact numerical values may acquire corrections. We have recomputed the dynamic transition with simplified energy-only landscapes (see Fig. 10). For 1-in-K SAT one can clearly see that the relative correction quickly diminishes. We believe that same happens for K-NAE SAT if sufficiently large K's are considered. If this indeed holds, it serves as a corroboration that our results are correct numerically for large K. It should be noted that the large-K limit corresponds to the so-called random energy model, where one does not expect to perform better then $O(2^N)$ via any quantum algorithm.

The idea of using energy-only landscapes was present in [30] as well as [31] and [32]. A jump in the time-dependence of the expected energy value was seen in numerical simulations [7], indicative of a first-order phase transition, though a different ensemble was considered (only instances having a unique solution were considered).

We also attempted to go beyond a simple annealing approximation and studied the dynamical transition using its refinement. For that we developed a polynomial mapping of the optimization problem defined on a full graph onto the problem defined on its subgraph (a core) where disorder-related fluctuations are significantly reduced and the annealing approximation is expected to perform much better. As a test we used the annealing approximation on a core to calculate the position γ_c of a static (satisfiability) transition where the entropy of the state with $E=0$ vanishes. We also computed γ_c numerically and found it to be very close to the analytical result. We then studied the dynamics of the quantum adiabatic evolution algorithm on a core using an extended set of landscape functions and found that the old results obtained on a full graph are reproduced qualitatively. This supports our earlier prediction that the location of the phase transition is not very sensitive to the exact nature of annealing approximation employed.

We emphasize that the different versions of the annealing approximation employed in this paper describe the phase transition as a global bifurcation between two macroscopic states (pure states) in the space of macroscopic variables defined by a set of landscape functions. The complexity is due to tunneling between the pure states. In contrast, spin glass theory predicts the existence of an infinite number of pure states [29] at sufficiently small energies. On the other hand, as we mentioned above, the first-order quantum phase transition occurs for large energies E_* and this has been con-

firmed with an improved annealing approximation.

Although the transition is seemingly absent for small K, a better approach (as compared to the annealing approximation) may reveal it. Moreover, we believe that if this happens the order of the transition will remain unchanged, suggesting that the disorder may be irrelevant for the determination of the order of the phase transition and, consequently, for the complexity of the quantum adiabatic algorithm. That is, the exponential complexity is not due to the true combinatorial complexity of the underlying random optimization problem but rather due to peculiarities of the driver term and a particular ensemble of random instances considered.

A future extension of the present work is to include a sufficiently large (possibly infinite) number of landscape parameters, thereby making the annealing approximation increasingly precise. In this regard we recall that the 1-bit-flip conditional distribution over landscape parameters employed in this paper (43) can be expressed via the set of coefficients $\{c_{\sigma,\mathbf{k}}\}$ that are concentrations of binary variables in a given string with different types $(\sigma,\mathbf{k})$ of an immediate neighborhood. In fact, these coefficients themselves can be used in an extended set of landscape parameters $\mathbf{x}$. Then an appropriate effective potential $f(\mathbf{x},\Gamma)$ can be introduced and its bifurcation can be studied when Γ varies from ∞ to 0. Furthermore, one can consider introducing progressively larger sets of landscape functions by defining neighborhoods of progressively larger size and using the well-known property that local structure of a random (hyper)graph is tree-like [33].

ACKNOWLEDGMENTS

This work was supported in part by the National Security Agency (NSA) and Advanced Research and Development Activity (ARDA) under Army Research Office (ARO) Contract No. ARDA-QC-P004-J132-Y03/LPS-FY2003. We also want to acknowledge the partial support of NASA CICT/IS program. We would also like to acknowledge helpful comments by E. Farhi, J. Goldstone (MIT) and S. Gutmann (Northeastern U).

APPENDIX: ON THE *NP*-COMPLETENESS OF POSITIVE 1-IN-*K* SAT AND POSITIVE *K*-NAE-SAT

There exists a huge class of *NP*-complete problems [1]. They possess a remarkable property: any instance of some *NP*-complete problem can be converted into an instance of some other *NP*-complete problem efficiently [that is the size of the new instance is bounded by the size of the original instance N raised to a finite power p (N^p), and the time needed to convert it is also polynomial in N].

For example the satisfiability problem and graph K-coloring problem are both *NP*-complete problems. For each boolean formula we can build a graph that is K-colorable if and only if the boolean formula is satisfiable, and vice versa. It follows that if a polynomial algorithm is invented to solve some *NP*-complete problem, it can be used to solve all *NP*-complete problems.

A central *NP*-complete problem is satisfiability. An instance of satisfiability is a set of clauses, where each clause is a "logical or" $(\vee)$ of literals, each literal being either some variable x or its negation $\neg x$. For any problem whose solution can be verified in polynomial time, one can construct an equivalent boolean formula. It is obvious for the problems at hand. The challenge now is to show that any boolean formula can be cast as some instance of either Positive 1-in-K-Sat or Positive K-NAE-SAT. It suffices to show that we need only encode basic boolean operations, e.g., $z=\neg(x\wedge y)$. We can trivially implement $\neg x=\neg(x\wedge x)$ and $z=x\vee y$ is implemented as $\neg(\neg x\wedge\neg y)$. Therefore, a clause of arbitrary length $(x_1\vee\cdots\vee x_K)$ can be represented as follows: $z_1=(x_1\vee x_2)$, $z_2=(z_1\vee x_3)$, up to $z=(z_{K-2}\vee x_K)$. Here z is *true* if and only if the clause is satisfied. By using $z=(x\wedge y)=\neg(\neg(x\wedge y))$ in a similar fashion we implement "logical and" $(\wedge)$ of all clauses. In the following we demonstrate how to encode the basic building blocks.

1. Positive 1-in-*K*-SAT

A clause of type $(x,\ldots,x,y)$ necessarily implies $x=0$ and $y=1$; hence we can represent constants 0 and 1. A clause of type $(0,\ldots,0,x,y)$ implies $x=\neg y$. Finally, a clause of type $(0,\ldots,0,x,y,z)$ is equivalent to a 3-clause (x,y,z) so that we can restrict ourselves to $K=3$ without losing generality.

For $K=3$, immediately observe that three clauses $(x,z,u')(y,z,u'')(u,u',u'')$ with free variables u, u', u'' imply $z=\neg(x\wedge y)$. This basic building block is in fact sufficient to build any boolean formula, as a result, any boolean formula can be cast as a 1-in-K SAT formula.

2. Positive *K*-NAE-SAT

A clause of type $(x,\ldots,x,y)$ necessarily implies $x=\neg y$, and $(x,\ldots,x,y,z)$ is equivalent to (x,y,z) so we once again restrict ourselves to $K=3$. In contrast to the 1-in-K problem, we shall require a nontrivial representation of *false* or *true*. We will use *pairs* of variables to denote variables of the boolean formula. Pairs 00 or 11 will represent value *false* and pairs 01 or 10 will represent *true*.

The next building block, $(x,y,t)(y,z,t)(z,x,t)$ ensures that $t=1$ if the majority of x,y,z are 0 and $t=0$ if the majority are 1. We shall use a shorthand $f(t;x,y,z)$ to denote this. The expression $f(z_1;x_1,y_1,y_2)f(z_2;x_2,y_1,y_2)$ then ensures $z=x\wedge y$ where x,y,z are represented as pairs x_1x_2, y_1y_2, z_1z_2 as indicated above. The operation of negation is trivial to represent: if $x\equiv x_1x_2$ then $\neg x\equiv(\neg x_1)x_2$. These two are sufficient to construct any boolean formula.

[1] R.M. Karp, in *Complexity of Computer Computations*, edited by R.E. Miller and J.W. Thatcher (Plenum, New York, 1972), pp. 85–103.
[2] S. Kirkpatrick, C.D. Gelatt, Jr., and M.P. Vecchi, Science **220**, 671 (1983).
[3] Y.T. Fu and P.W. Anderson, J. Phys. A **19**, 1605 (1986).
[4] M. Mezard, G. Parisi, and R. Zecchina, Science **297**, 812 (2002).
[5] E. Farhi, J. Goldstone, S. Gutmann, and M. Sipser, e-print quant-ph/0001106.
[6] E. Farhi, J. Goldstone, S. Gutmann, J. Lapan, A. Lundgren, and D. Preda, Science **292**, 472 (2001).
[7] T. Hogg, Phys. Rev. A **67**, 022314 (2003).
[8] S. Lloyd, Science **273**, 1073 (1996).
[9] W.M. Kaminsky and S. Lloyd, in *Quantum Computing & Quantum Bits in Mesoscopic Systems* (Kluwer Academic, Dordrecht, 2003); see also e-print quant-ph/0211152.
[10] A.M. Childs, E. Farhi, J. Goldstone, and S. Gutmann, Quantum Inf. Comput. **2**, 181 (2002).
[11] J. Brooke, D. Bitko, T.F. Rosenbaum, and G. Aeppli, Science **284**, 779 (1999).
[12] G.E. Santoro, R. Martonak, E. Tosatti, and R. Car, Science **295**, 2427 (2002).
[13] J. Brooke, T.F. Rosenbaum, and G. Aeppli, Nature (London) **413**, 610 (2001).
[14] E. Farhi, J. Goldstone, and S. Gutmann, e-print quant-ph/0201031.
[15] Y. Boufkhad, V. Kalapala, and C. Moore (unpublished).
[16] G. Semerjian and R. Monasson, Phys. Rev. E **67**, 066103 (2003).
[17] P. Cheeseman, B. Kanefsky, and W.M. Taylor, Proceedings of the International Joint Conference on Artificial Intelligence, 1991, Vol. 1, pp. 331–337.
[18] S. Kirkpatrick and B. Selman, Science **264**, 1297 (1994).
[19] Artif. Intell. **81**, 1–2 (1996), special issue on topic, edited by T. Hogg, B.A. Huberman, and C. Williams.
[20] W. Barthel, A.K. Hartmann, and M. Weigt, Phys. Rev. E **67**, 066104 (2003).
[21] A. Messiah, *Quantum Mechanics* (North-Holland, Ansterdam, 1966), Vol. 1.
[22] W. Van Dam, M. Mosca, and U. Vazirani, Proceedings of the 42nd Annual Symposium on Foundations of Computer Science; see also e-print quant-ph/0206003.
[23] E. Farhi, J. Goldstone, and S. Gutmann, e-print quant-ph/0208135.
[24] A. Boulatov and V.N. Smelyanskiy, Phys. Rev. A **68**, 062321 (2003); see also e-print quant-ph/0309150.
[25] R. Monasson and R. Zecchina, Phys. Rev. Lett. **76**, 3881 (1996).
[26] R. Monasson and R. Zecchina, Phys. Rev. E **56**, 1357 (1997).
[27] M. Mezard, F. Ricci-Tersenghi, and R. Zecchina, J. Stat. Phys. **111**, 505 (2003).
[28] S. Knysh, V. Smelyanskiy, and R.D. Morris, e-print cond-mat/0403416.
[29] *Spin Spin Glass Theory and Beyond*, edited by M. Mezard, G. Parisi, and M.A. Virasoro (World Scientific, Singapore, 1987).
[30] T. Hogg, Phys. Rev. A **61**, 052311 (2000).
[31] W. Macready (unpublished).
[32] V. Smelyanskiy, U. Toussaint, and D. Timucin, e-print quant-ph/0202155.
[33] M. Mezard and G. Parisi, J. Stat. Phys. **111**, 1 (2003).